Metals and Their Scaffolds To Promote Difficult Enzymatic Reactions

Stephen W. Ragsdale*

Department of Biochemistry, Beadle Center, University of Nebraska, Lincoln, Nebraska 68588-0664

Received January 19, 2006

Contents

1. Introduction and Overview

1.1. Historical Background

1.1.1. Metal Ions and Their Scaffold To Promote Reactions

Approximately one-third of the known enzymes are metalloenzymes. The metal ions promote a variety of reactions in these enzymes, including bond cleavage and formation, electron transfer, atom transfer, and radical chemistry. The reactions catalyzed are essential for DNA synthesis, cell replication, cellular energy production, O_2 generation (via photosynthesis), sensing, and transporting, as well as O_2 activation for reaction with a myriad of organic molecules. In addition, metalloenzymes are both the source of reactive oxygen species and a major means by which our body protects us from these potentially devastating molecules.

There was a heated debate around the turn of the 20th century about whether the role of the protein "scaffold" was catalytic or structural. One of the major apparent triumphs for the "catalytic camp" in this argument was the crystallization of urease, which was concluded in 1926 to contain only amino acids.[1] It is ironic that in 1975, urease was found to also contain catalytically active nickel.[2]

1.1.2. The Scaffold and the Metal: Common Scaffolds for Uncommon Reactions

This review focuses on how metal ions and their scaffolds promote difficult biochemical reactions. What do I mean by a scaffold? In the context of a metalloenzyme, a scaffold can be defined as a framework of atoms and bonds that supports the activity of the metal ion. Thus, a scaffold includes the primary coordination sphere of ligating atoms

Stephen W. Ragsdale is the Charles Bessey Professor of Biochemistry at the University of Nebraska. He was born in Rome, GA, in 1952 and received his B.S. and Ph.D. degrees in Biochemistry from the University of Georgia, where he began research in Microbial Biochemistry and Enzymology with Dr. Lars Ljungdahl. After graduating in 1983, he was an NIH Postdoctoral Associate with Harland G. Wood at Case Western Reserve University in Cleveland, OH. In 1987, he joined the Chemistry faculty at the University of Wisconsin-Milwaukee, where he was a Shaw Scholar. He joined the Biochemistry Department at the University of Nebraska as Associate Professor in 1991 and became full Professor in 1996 and Bessey Professor in 2003. His research interests span the areas of microbial and environmental biochemistry, metallobiochemistry, and enzymology. His hobbies include music and literature.

* To whom correspondence should be addressed. Email: sragsdale1@unl.edu.

10.1021/cr0503153 CCC: $59.00
Published on Web 07/15/2006

(usually sulfur, oxygen, and nitrogen) that are directly attached to the metal ion. Inorganic chemists attempting to model the reactivity of a metalloenzyme typically synthesize complexes that closely match those identified by spectroscopic or X-ray crystallographic studies because of the important role that the coordination complex plays in controlling the reactivity of the metal ion. These coordinating ligands often specify which metal ion can bind to the enzyme as well as control which oxidation state and/or spin state can be accessed. For example, in nitrile hydratase, an unusual primary coordination sphere consisting of two peptide amide nitrogens and three cysteinate sulfurs stabilizes iron or cobalt in their rarely encountered low spin +3 state.[3] Similarly, the central cavities of the tetrapyrroles in corrin and hydrocorphin are tailored for only particular metal ions and oxidation states, for example, low spin cobalt (I, II, and III) in cobalamin, and the larger nickel ion in the tetrahydrocorphinoid Coenzyme F_{430}.[4] The primary coordination sphere can fine-tune and enhance (or dampen) the reactivity of the metal ion. In several enzymes (nitrile hydratase, superoxide reductase, and peptide deformylase), a cysteinate trans to the substrate binding site appears to control reactivity of the ferric ion.[3]

In building construction, scaffolds are usually temporary structures; likewise, particular ligands sometimes move as in the carboxylate shift during the ribonucleotide reductase[5,6] and methane monooxygenase reactions.[7] In other cases, the ligands release from the metal ion during the course of a reaction; for example, tyrosine releases from the metal during the 3,4-protocatechuate dioxygenase reaction, which allows the substrate to bind in the reactive dianion chelate form.[8] Other examples of ligand release, described by Frazee et al.,[8] include Gln release when substrate binds to isopenicillin-*N*-synthase,[9] oxo ligand release when DMSO reductase undergoes reduction,[10] and ligand switches at both hemes of nitrite reductase (His to Met in the c heme and Tyr to nitrite in the d heme).[11]

The secondary coordination sphere, which includes atoms that are near (but not directly attached to) the metal ion, can be considered as part of the scaffold, since the properties of these atoms can strongly influence the reactivity of the metal ion. A counterion, for example, might be included in the second coordination sphere of the metal ion. The substrates for a metalloenzyme often are contained within the metal ion's second coordination sphere. Recent studies have shown that second coordination sphere effects strongly influence the kinetics and themodynamics of catalysis by the Fe and Mn superoxide dismutases.[12,13] Likewise, second sphere effects are important in controlling dioxygen binding to hemerythrin[14] and myoglobin,[15] and conformational flexibility in lipoxygenase.[16]

The scaffold could also be broadly defined as the protein that provides the overall supporting framework for the metal ion. In this review, we will focus primarily on the catalytic contribution of the metal ion and its first coordination sphere in promoting catalysis of difficult reactions and, in some cases, include key features contributed by the extended scaffolding network of the second coordination sphere and the protein environment itself.

The first and second coordination spheres, as well as the extended protein scaffold, have major effects on the properties of carbonic anhydrase.[17] For example, the three neutral histidine ligands in the first coordination sphere of carbonic anhydrase are key in lowering the pK_a of Zn-bound water from 10 to 6.8, allowing the formation of the catalytic intermediate Zn^{2+}-OH at physiological pH. Replacing these residues with negatively charged residues causes a significant increase in this pK_a value and decrease the catalytic efficiency by greater than 1000-fold.[18] The tetrahedral (3 His, 1 OH) nature of the active site also plays a key role in optimizing the electrostatic effect of Zn in promoting its Lewis acid activity and enhancing catalysis.[19] The second sphere ligands play a key role in carbonic anhydrase structure and function by providing a hydrogen bonding network that correctly positions the His residues in the first coordination sphere. Disruption of each specific H-bond causes a 10-fold decrease in the affinity of the enzyme for Zn. An important H-bond is also made from a second sphere Thr residue to the Zn-bound water, and replacement of the Thr by Ala results in a 100-fold decrease in catalytic activity and a 1 unit shift in the pK_a of the water ligand.[20] The effect of the extended scaffold on Zn binding to carbonic anhydrase has also been examined. For example, substitution of the aromatic residues within the hydrophobic core near the Zn site markedy affects Zn affinity.[21]

1.1.3. What Are Difficult Reactions?

In the title and throughout this review, the term "difficult reactions" describes reactions with significant kinetic and/or thermodynamic barriers. Enzymes and their prosthetic groups can only lower the kinetic barrier, not influence the overall reaction thermodynamics. A particular step in a difficult solution reaction with a tremendous activation barrier usually occurs in several steps with significantly lowered activation energies. This occurs because the enzyme usually catalyzes the overall transformation by a different mechanism than that used in solution. The enzymatic reaction involves more steps (and often coupled steps) and employs binding energy, acid−base catalysis, covalent catalysis, and so forth, to facilitate the reaction. For example, I will describe a number of reactions that take advantage of some unique properties of metals to scale extremely high activation barriers (for the solution reaction).

Another way to view how an enzyme deals with a difficult reaction is to consider its transition state and how tightly this transition state structure should bind to the enzyme. Thus, to achieve a large-fold rate enhancement, the enzyme should exhibit a correspondingly low dissociation constant for the transition state structure. For example, a transition state analogue of the orotidine 5′-phosphate decarboxylase, which has been honored with the title of the most proficient enzyme because it accomplishes a 10^{23}-fold rate enhancement, has been designed that exhibits a binding constant of 9×10^{-12} M.[22] The active site contains numerous H-bonding and salt-bridge contacts that stabilize this transition state analogue.[23] Often, the substrate (or transition state) for a metalloenzyme has functionalities that resemble the coordination complexes preferred for the active site metal ion in solution; in these cases, the metal ion will be particularly well-suited for binding that substrate. Similarly, the active site of the enzyme usually contains ideal chelating groups (the primary scaffold) to bind the metal ion tightly. Accordingly, reaction rates can be controlled by variation of the metal ion, the scaffold, or the redox state of a particular metal ion.

Since the overall reaction cannot occur faster than the rate at which substrate and catalyst can collide, the ranking of catalytic proficiency by comparing the uncatalyzed and catalyzed reactions is somewhat misleading. One could imagine an enzyme that promotes a tremendous rate en-

hancement of a very slow reaction, yet the rate might still be slower than the diffusion-controlled rate, which in aqueous solution for enzyme-sized molecules is 10^8-10^9 M^{-1} s^{-1}. Thus, there would still be room for evolutionary improvement of such an enzyme. Nature would be expected to select for catalytic machinery that allow an enzyme-catalyzed reaction to reach the diffusion-controlled rate. In this review, I will focus on how the metal sites in enzymes can enhance the rates of particularly difficult reactions and the principles by which several well-studied metalloenzymes approach diffusion-controlled rates. The reactions that will be described involve the metal-catalyzed generation of potent electrophiles, nucleophiles, and radicals.

2. Metals and Their Scaffolds: Selected Examples

2.1. Metals To Promote Radical Reactions

Radicals are highly reactive chemical species and, thus, are used to catalyze reactions with high activation energy thresholds. The involvement of radicals in the enzymatic mechanisms of ribonucleotide reductase,[24] pyruvate:ferredoxin oxidoreductase,[25] and several *S*-adenosyl-methionine-dependent[26] and adenosylcobalamin-dependent[27−30] enzymes has been reviewed. A thematic review on radical enzymology appeared in 2003.[31]

When an enzyme introduces a catalytic radical into the active site of a protein, it can undergo stabilization by abstracting a hydrogen atom from the substrate. Hence, the high reactivity of the catalytic radical has been transferred to the substrate, which then can undergo its subsequent reactions with enhanced ease. For a reaction with a very high transition state barrier, generation of the catalytic radical can be the most difficult (slowest) step with the subsequent steps being quite facile (fast). Several principles make this mode of catalysis particularly efficient. By coupling the generation of the catalytic radical to hydrogen atom abstraction from the substrate, the energy barrier for radical generation is significantly reduced. Thus, the primary radical is quenched, while the radical is propagated through the catalytic cycle; then, the catalytic radical is regenerated at the end of each turnover. Notably, this strategy would only be effective if the reaction is not reversible.

Radicals in enzymes include the adenosyl radical, generated by cofactor-derived radicals, including adenosylcobalamin, adenosylhomocysteine, heme, flavin, and tetrahydrobiopterin. A number of enzymes contain protein-derived radicals including cysteinyl (thiyl, found in Type I, II, and III ribonucleotide reductases), glycyl (pyruvate formate-lyase, Type III anaerobic ribonucleotide reductase, and benzylsuccinate synthase), tyrosyl (many including prostaglandin synthase, galactose oxidase, ribonucleotide reductase), and tryptophanyl (cytochrome *c* peroxidase) radicals. The first protein radical identified was the tyrosyl radical in ribonucleotide reductase.[32] Others contain substrate-derived radicals that are stabilized by cofactors such as the hydroxyethylthiamine pyrophosphate radical or the series of radicals bound to pyridoxal phosphate in the lysine-2,3-aminomutase reaction. The metal centers (binuclear Fe, FeS clusters, mononuclear Cu, Co) in metalloenzymes are involved in most, if not all, of these reactions either at the initiation state or in stabilization of the catalytic radical.

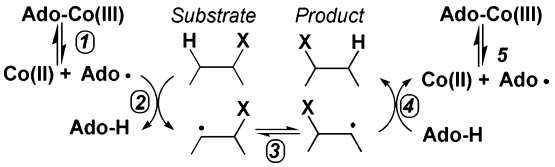

Figure 1. Simplified mechanism of an adenosylcobalamin-dependent isomerase reaction.

2.1.1. Metals and Adenosyl Radicals: Rich Man-Poor Man Saga—SAM and Adenosylcobalamin

2.1.1.1. The Organometallic Chemistry Of Adenosylcobalamin in Promoting Radical Reactions. The principles just described are illustrated in the simplified scheme for a rearrangement reaction catalyzed by an adenosylcobalamin-dependent isomerase (Figure 1). In these reactions, the metal (cobalt) is key in stabilizing a reactive and transient radical that forms during the catalytic cycle. Adenosylcobalamin undergoes homolytic cleavage to form Co(II) and a carbon-centered adenosyl radical (Step 1). This process is rather like that of a zymogen, which is latent until a bond cleavage occurs to unmask the active catalyst; however, in this case, the latent radical is unleashed when the organometallic bond is cleaved. The bond dissociation energy of the Co−C bond is approximately 142 kJ/mol,[33,34] and the rate of Co−C bond cleavage is enhanced by 1 trillion-fold relative to the noncatalyzed reaction.[33] There is an inherent protective mechanism in this scheme—when the Co−C bond is cleaved in the absence of substrate, radical recombination can occur to regenerate the adenosylcobalamin. In Step 2, the radical reaction propagates when the adenosyl radical abstracts a hydrogen atom from the substrate to generate a substrate radical and adenosine. There is evidence that the steps of Co−C bond cleavage and H-atom abstraction are coupled in several Ado-Cbl-dependent isomerases based on the significant effect of substrate deuteration on the rate of Co−C bond cleavage.[35−37] In addition, very large kinetic isotope effects were observed, indicating that kinetic coupling as well as H-atom tunneling control the trajectory of these radical reactions. In glutamate mutase, the isotope effects (of 28) and the effect of substrate deuteration on Co−C bond cleavage[38] have been recently reinterpreted, and H-atom tunneling or kinetic coupling are no longer necessary to explain the results.[39] Following H-atom abstraction, the substrate radical then rearranges to form a product radical (Step 3) that reabstracts the hydrogen atom from adenosine to yield the product and reform the adenosyl radical (Step 4), which can undergo another round of H-atom abstraction from the substrate or recombine with cobalt to regenerate adenosylcobalamin (Step 5). In these reactions, the metal ion (Co) is thought to play a role in maintaining a reservoir of the latent adenosyl radical; however, it is not involved directly in the chemistry of the rearrangement reaction. Thus, the metal ion has been termed a "bystander" in these reactions. Perhaps the most remarkable adenosylcobalamin-dependent rearrangement reaction is catalyzed by glutamate mutase, where a saturated carbon (a glycyl moiety) migrates from C-3 to C-4 of glutamate to form methylaspartate (Figure 2). There is relatively strong evidence that this reaction may not occur by a simple migration, but that glutamate may undergo a fragmentation into acrylate and a glycyl radical followed by reassociation.[40]

The adenosyl radical generated from adenosylcobalamin is used by isomerases that catalyze carbon skeleton rearrangements (methylmalonyl-CoA mutase, glutamate mutase,

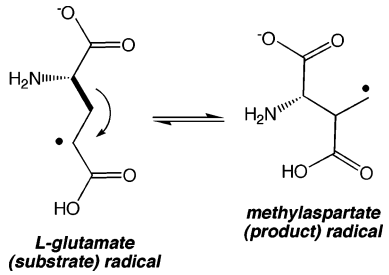

Figure 2. Rearrangement catalyzed by glutamate mutase.

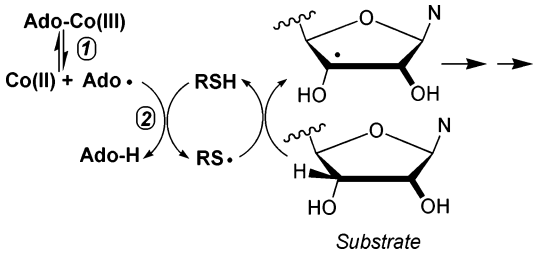

Figure 3. Adenosyl radical generation of a thiyl radical.

methyleneglutarate mutase, and isobutyryl-CoA mutase),[41] isomerases that catalyze heteroatom (OH, NH_2) migrations (diol dehydratase, glycerol dehydratase, ethanolamine ammonia lyase),[27] and Class II ribonucleotide reductase.[42] In all these cases, the adenosyl radical functions in hydrogen atom abstraction. For the isomerases, the hydrogen atom is abstracted from the substrate, while for ribonucleotide reductase, it abstracts the hydrogen atom from an active site cysteine residue generating a thiyl radical, which then abstracts the hydrogen from the ribonucleotide (Figure 3). All three classes of ribonucleotide reductase generate a thiyl radical and bind their substrates in a 10-stranded $\alpha\beta$ barrel fold.[43] Thus, in the ribonucleotide reductases, it appears that different metal-dependent radical generation modules interface with a common and evolutionarily ancient thiyl radical/substrate binding domain.

2.1.1.2. Metals in Promoting the Reactions of Radical SAM Enzymes. Metals are also involved in generating the adenosyl radical in a class of *S*-adenosylmethionine-dependent enzymes, the so-called "radical SAM enzymes." Several reviews of radical SAM proteins have recently appeared,[26,44−46] including a recent one focused on spectroscopic methods that have been used to characterize this class of proteins.[47] SAM acts as a methyl donor in methyltransferases, but its role is similar to that of adenosylcobalamin in the radical SAM enzymes (Figure 4). In this case, the metal, a $[4Fe-4S]^{2+/1+}$ cluster, serves as a one-electron donor. The Class III ribonucleotide reductase is a radical SAM enzyme. Replacement of reaction 1 in Figure 3 with SAM plus a reduced $[4Fe-4S]^{1+}$ cluster generates the oxidized (2+) state of the cluster and the Ado radical, which will then directly abstract a hydrogen atom from an active site cysteine leading to the formation of a thiyl radical exactly as in the adenosylcobalamin-dependent ribonucleotide reductase.[43]

On the basis of a bioinformatics approach, there appear to be at least 600 radical SAM enzymes in archaea, bacteria, plants, and animals, which share a distinct iron−sulfur motif, CXXXCXXC, and a glycine-rich region.[48] The Cys-rich region and the Gly-rich (GxIxGxxE) region are located within an $(\alpha\beta)_6$ TIM barrel-like domain.[49] The radical SAM enzyme family includes lysine 2,3-aminomutase, which is unusual in the generation of a substrate-derived radical adduct with pyridoxal phosphate; biotin synthase and lipoic acid synthase, which insert sulfur into these vitamins; and the activating proteins for pyruvate formate-lyase and the Type III ribonucleotide reductase activating protein, which generate a glycyl radical. The bioinformatics search also identified proteins involved in pathways for the biosynthesis of antibiotics, herbicides, thiamin, heme, chlorophyll, molybdopterin, the nitrogenase MoFe cofactor, and pyrroloquinoline quinone.[48]

Spectroscopic and crystallographic studies demonstrate that SAM binds directly to the FeS cluster as shown in Figure 4, with the amino and carboxylate groups of methionine chelating one of the iron atoms in the cluster. In pyruvate formate lyase activating protein, there is evidence that the thioether sulfur of methionine bound to one of the inorganic sulfur atoms of the cluster, indicating that the radical is stabilized by interactions with the metal center.[48,50] This interaction between the sulfide in the cluster and the sulfur atom of SAM has been speculated to help trigger the reductive cleavage of the C−S bond to generate the adenosyl radical.[50]

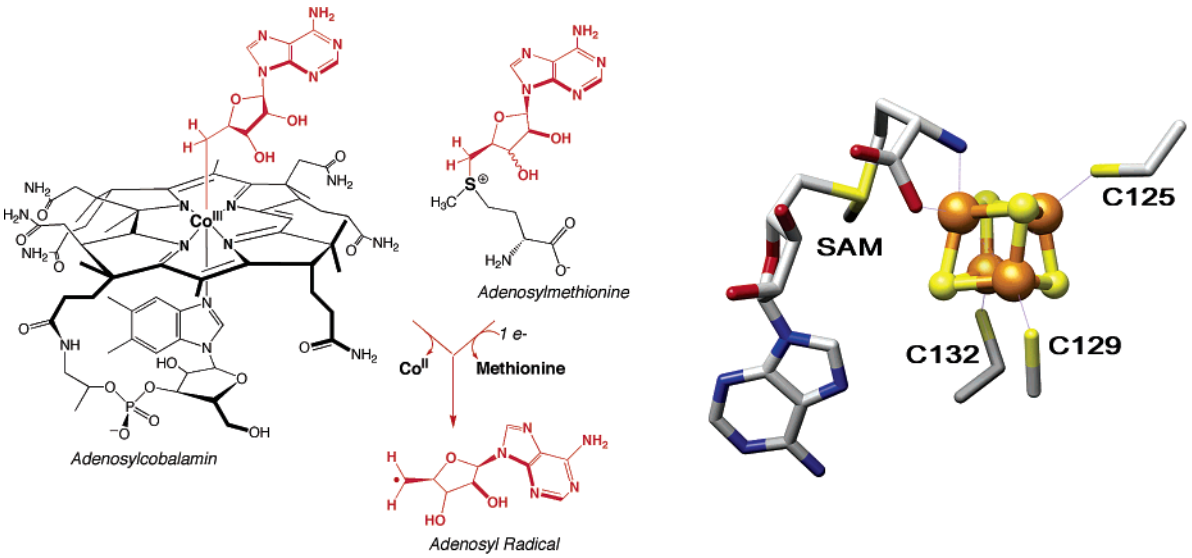

Figure 4. Adenosyl radical generation in the adenosylcobalamin and radical SAM enzymes (left panel). Coordination of SAM to the FeS cluster in SAM radical enzymes (right panel) based on the structure of lysine-2,3-aminomutase.[48] Drawn from PDB no. 2A5H.

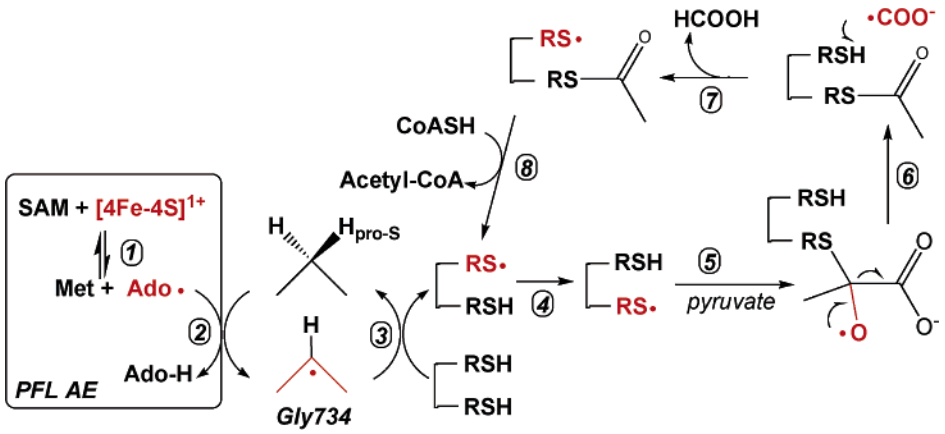

Figure 5. PFL activation and mechanism. Radicals are shown in red.

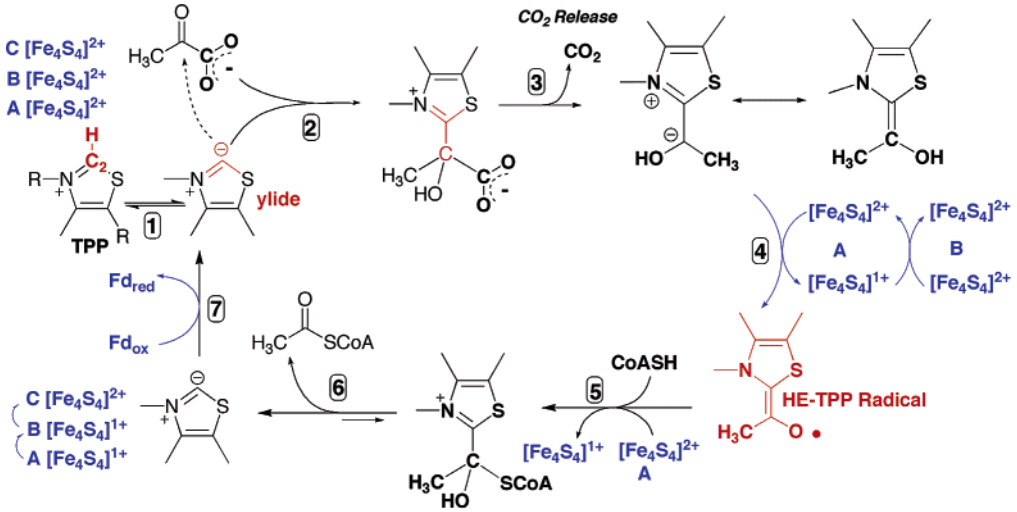

Figure 6. Proposed mechanism of PFOR. Radical reactions are shown in blue, and the reactive C-2 of TPP and the HE-TPP radical intermediate are shown in red.

Pyruvate formate lyase (PFL, EC 2.3.1.54) is a radical enzyme that utilizes a glycyl and a thiyl radical during catalysis.[51] The freely reversible conversion of pyruvate and CoA to formate and acetyl-CoA in the PFL reaction cycle occurs with a turnover number of 770 s^{-1} and $k_{cat}/K_{m(pyruvate)}$ of 3.3×10^5 M^{-1} s^{-1} at 30 °C ($K_{m(pyruvate)}$, 2 mM; K_m CoA, 0.0068 mM).[52] Formation of the glycyl radical is catalyzed by the SAM radical enzyme, PFL activating enzyme. The glycyl radical is relatively stable and has been characterized in detail.[53] The overall activation and catalytic cycle are outlined in Figure 5, which highlights the eight radicals formed during the reaction (shown in red boldface type). The adenosyl radical, which is generated on PFL-activating enzyme by reductive cleavage of the C−S bond as described above (Step 1), directly abstracts a hydrogen atom from an active site glycine residue of PFL to generate the glycyl radical (Step 2). In Step 3, the glycyl radical abstracts a hydrogen atom from a nearby cysteine residue (Cys419) to form a thiyl radical. The radical is then transferred to the vicinal cysteine (Cys418) (Step 4), which undergoes acetylation by reacting with pyruvate to form a lactoyl radical intermediate (Step 5). In Step 6, carbon−carbon bond homolysis yields a carboylate anion radical and an acetylated Cys418. A carboxylate radical is very reactive and is proposed to react with the free Cys419 to regenerate a thiyl radical, which can either re-enter the catalytic cycle or react with glycine to regenerate the glycyl radical, which would subsequently regenerate the thiyl radical.

2.1.2. Thiamine Pyrophosphate-Dependent Radical Reactions: Pyruvate Ferredoxin Oxidoreductase and Pyruvate Oxidase

Pyruvate:ferredoxin oxidoreductase (PFOR) catalyzes a reaction that is similar in many respects to PFL: the thiamine pyrophosphate (TPP)-dependent oxidative decarboxylation of pyruvate to form acetyl-CoA and CO_2.[25] Similarities include the substrates (pyruvate, CoA) and one of the products (acetyl-CoA) and the involvement of [4Fe−4S] clusters and radicals in the mechanism. However, instead of SAM, PFOR uses TPP as a coenzyme in a reaction that could be described as a mechanistic convergence of an electrophilic TPP reaction module characteristic of transketolase and pyruvate dehydrogenase with a rapid electron-transfer module characteristic of many iron−sulfur proteins. Like many of the radical systems described in this section, the metal center is involved in generating and stabilizing the radical center, but in a manner that does not involve kinetic coupling to a hydrogen abstraction step as in the adenosyl radical systems. PFOR is related to various α-ketoacid oxidoreductases

The mechanism of the PFOR-catalyzed reaction (Figure 6) begins, without the involvement of redox-active metals, like the mechanistically similar early steps in the reactions of pyruvate dehydrogenase, pyruvate oxidase, and pyruvate decarboxylase. There is a remarkable acid−base reaction (Step 1) in which, as Ron Breslow discovered in 1962, carbon 2 of the thiazolium ring (with a pK_a of 17−19![54]) of

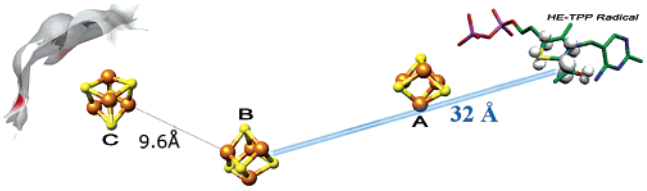

Figure 7. Redox centers in PFOR based on the crystal structure (1KEK)[62] and showing the spin density on the radical (spin density is proportional to the size of the balloon-like orbital) based on recent spectroscopic and computational studies.[63] Drawn using Chimera.

TPP undergoes deprotonation[55,56] to generate an ylide, which is a highly reactive thiazolium anion that is resonance-stabilized by charge delocalization among the various atoms in the aromatic thiazole ring. However, it is the thiazolium anion shown in Figure 6 that catalyzes a nucleophilic attack on the C2 atom of pyruvate, generating a lactoyl-TPP adduct (Step 2). This adduct then undergoes decarboxylation (Step 3) to generate the 2α-hydroxyethylidene-TPP (HE-TPP) intermediate.

The HE-TPP intermediate is a highly reactive α-carbanion ("active aldehyde") and will exist in this charged state when the hydroxy and methyl groups are arranged perpendicular to the plane of the thiazolium ring.[57] The zwitterionic form is in equilibrium with the neutral resonance-stabilized enamine; thus, the transition state corresponding to this intermediate would likely have a structure between the enamine (to stabilize the high-energy state) and the α-carbanion (to maximize reactivity) form. All the TPP enzymes generate this intermediate, and beyond this step, the reactions of transketolase, pyruvate dehydrogenase, pyruvate decarboxylase, and PFOR/pyruvate oxidase diverge.

In pyruvate decarboxylase, the intermediate is protonated to produce acetaldehyde, while in transketolase, it reacts with a second ketose. As shown in Step 4, in PFOR, HE-TPP transfers one electron to a [4Fe−4S] cluster, presumably Cluster A, which is closest, transforming it from the 2+ to the 1+ state and generating the HE-TPP radical intermediate (shown in red). It is the presence of an electron sink (a "redox wire") near the negative charge of HE-TPP in PFOR and pyruvate oxidase that poises the reaction for radical chemistry (Figure 7). In PFOR, the wire consists of three [4Fe−4S] clusters,[58,59] while in pyruvate oxidase, it is a flavin center.[60] Recent studies indicate that he electron is further transferred from Cluster A to Cluster B, which reoxidizes Cluster A and prepares it for the next one-electron-transfer reaction.[61] Cluster C is near the surface of the enzyme, where it can transfer electrons to external mediators, like ferredoxin. Thus, one role of the metal cluster is to oxidize the HE-TPP intermediate, thus, initiating the radical reaction. This electron transfer-driven process is fundamentally different from the hydrogen atom abstractions normally encountered in radical reactions.

The structure of the HE-TPP radical has been under recent scrutiny. On the basis of X-ray crystallographic studies of PFOR partly in its radical state, the structure of the HE-TPP radical was proposed to be a σ-type radical (Figure 8).[62] Unusual characteristics of this radical include ketonization of the hydroxy group at position C2α to form an acetyl radical, a long C2−C2α bond, sp^3 hybridization at thiazolium atoms N3 and C5, and tautomerization of the C4−C5 double bond to give an exocyclic double bond. This was a surprising proposal, since it had been described previously as a π-type radical benefiting from stabilization among at least seven different resonance forms (though only one is shown in the figure).[64] One major difference between the two models is where the electron spin lies. The σ radical would have highly localized spin at the C-2 carbon of the HE group, while in a π radical, the spin would be delocalized among the atoms of the HE group and the thiazole ring. Recent spectroscopic results clearly demonstrate a spin-delocalized model, casting doubt on the σ-radical formulation and providing evidence supporting a π-type radical.[63]

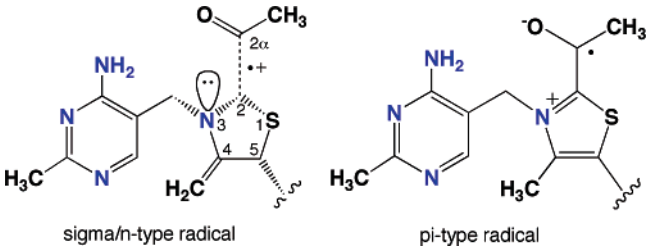

Figure 8. Differences between the σ and π radicals.

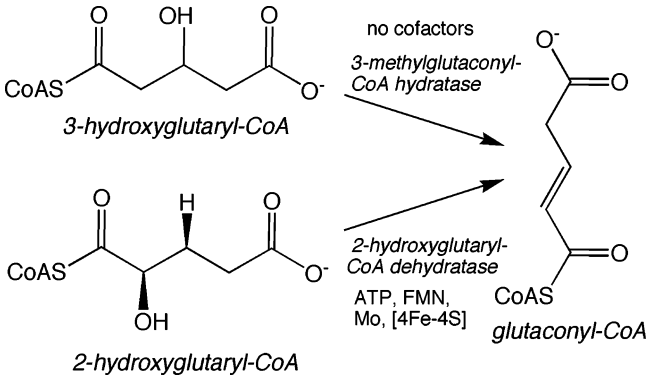

Figure 9. Comparison of two reactions that form glutaconyl-CoA.

2.1.3. Metals, Radicals, and Herculean Acid–Base Tasks

A last radical reaction will be examined in this section: the 2-hydroxyglutaryl-CoA dehydratase catalyzed dehydration of (*R*)-2-hydroxyglutaryl-CoA to form (*E*)-glutaconyl-CoA (Figure 9). Study of this reaction is instructive when considering when Nature uses radical chemistry, especially when compared with the reaction of 3-methylglutaconyl-CoA hydratase.[65,66] These enzymes catalyze what appear to be similar hydration/dehydrations reactions; however, one of these (2-hydroxyglutaryl-CoA dehydratase) utilizes radical chemistry, while the other catalyzes a rather routine hydration/dehydration reaction.

The 2-hydroxyglutaryl-CoA dehydratase catalyzed radical reaction is difficult because the hydrogen at carbon 3 of 2-hydroxyglutaryl-CoA, which must be removed as a proton, is unactivated and has a pK_a value near 40.[67,68] The enzyme appears to overcome this hurdle by generation of an enoyl radical (Figure 10), which decreases the pK_a of the C3 proton to approximately 14.[68] Therefore, initiation of this radical chemistry results in a 10^{26}-fold lowering of the kinetic barrier to deprotonation.

Radical chemistry is not envisioned for the "easy" reaction catalyzed by 3-hydroxyglutaryl-CoA dehydratase (3-methylglutaconyl-CoA hydratase). This reaction involves polarization of the double bond of glutaconyl-CoA, then addition of a hydroxyl group to a positively charged α-carbon and a proton to the negatively charged β-carbon to generate 3-hydroxyglutaryl-CoA. Thus, the hydration/dehydration of 3-hydroxyglutaryl-CoA probably occurs through standard acid−base chemistry in the active site.

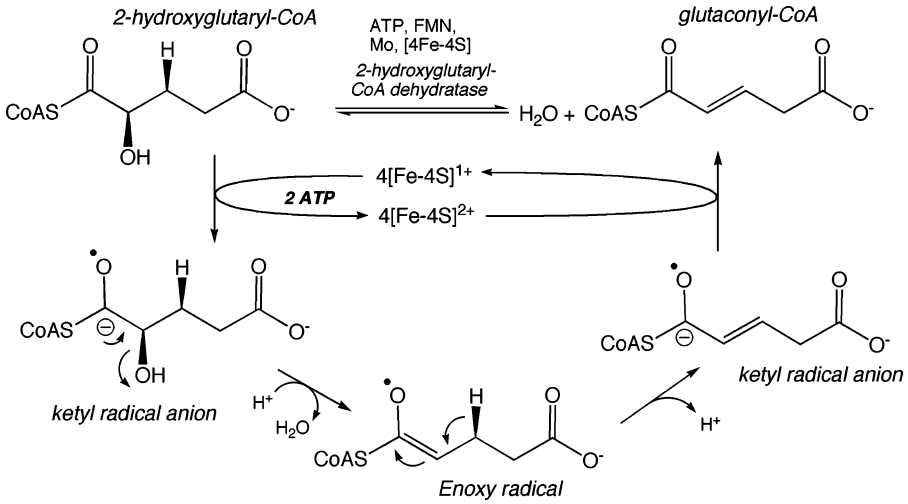

Figure 10. Proposed radical mechanism of 2-hydroxyglutaryl-CoA dehydratase based on Buckel et al..[68]

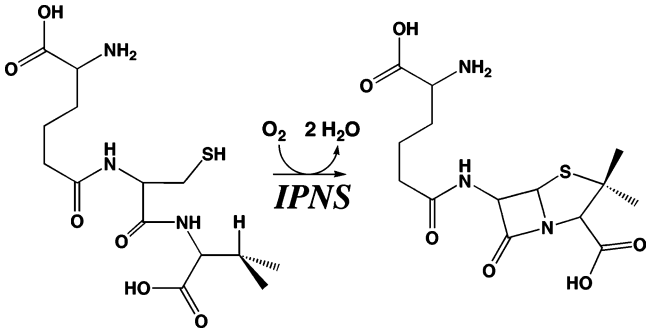

Figure 11. Reaction catalyzed by isopenicillin-*N*-synthase.

2.2. Metals and Their Scaffolds To Catalyze Reactions Involving O_2

A variety of mechanisms and metals are utilized to catalyze reactions involving oxygen. This section describes several classes of such enzymes. A recent review is available describing how iron activates oxygen.[69]

2.2.1. Metalloenzymes Containing a 2-His-1-Carboxylate Facial Triad Motif

There is a large class of metalloenzymes that contain a 2-His-1-carboxylate facial triad motif.[70] All of these enzymes contain a single metal ion that is octahedrally coordinated by two His and one Asp or Glu residues and includes a large number of enzymes that are involved in diverse oxygenation reactions including the 2-oxoacid-dependent enzymes, pterin-dependent hydroxylases, catechol dioxygenases (Fe and Mn), Rieske dioxygenases, isopenicillin-*N*-synthase, and the ethylene-forming enzyme 1-aminocyclopropane-1-carboxylic acid oxidase.[70,71] These are complex and difficult reactions involving the oxygenolytic cleavage of catechols, the hydroxylation and dihydroxylation of aromatics, the synthesis of ethylene from aminocyclopropane-1-carboxylic acid, and a complex transformation leading to the synthesis of penicillin (Figures 11 and 12).

Among the iron-containing proteins of this class, there is substantial divergence in reaction mechanism, especially related to the redox chemistry involved in catalysis. For example, ring cleaving dioxygenases such as protocatechuate 3,4 dioxygenase apparently remain in the Fe^{3+} state throughout the catalytic cycle,[8] while naphthalene dioxygenase appears to utilize an Fe(V)═O species, although there is some

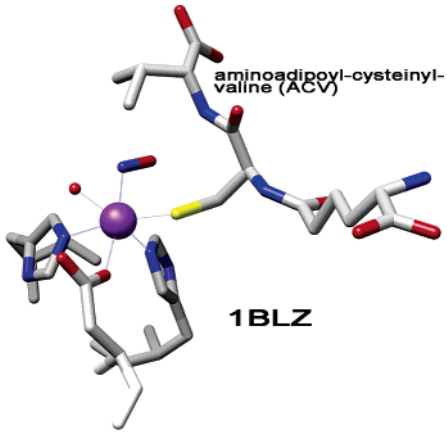

Figure 12. Structure of isopenicillin-*N*-synthase with bound NO and ACV.[9] Generated from PDB no. 1BLZ using Chimera.

evidence from computational studies of naphthalene dioxygenase for reaction of the Fe-peroxy species on the substrate.[72] On the other hand, in taurine dioxygenase (TauD) and other α-ketoglutarate-dependent enzymes, there is significant evidence supporting O−O bond cleavage, which leads to a reactive Fe(IV)═O species that reacts with the substrate.[71,72]

TauD is an α-ketoglutarate-dependent enzyme that catalyzes the hydroxylation of taurine (2-amino-1-ethanesulfonate) to form 1-hydroxytaurine (2-amino-1-hydroxy-1-ethanesulfonate). This reaction is instructive because it involves the metal, two different substrate complexes, and a recognized high valent intermediate. As shown in Figure 13, substrate (taurine and α-ketoglutarate) and then molecular oxygen bind to the 5-coordinate (2-His-1-carboxylate facial triad) Fe^{2+} center in the enzyme. Binding of taurine increases the affinity for α-ketoglutarate by 15-fold.[73] Figure 12 shows the likely orientation of substrate and dioxygen in the oxy−Fe^{2+} complex, based on the X-ray crystal structure of isopenicillin-*N*-synthase with NO and substrate bound.[9] In the TauD mechanism, the next step is an internal redox reaction that leads to the formation of first an iron−peroxo (not shown) complex that attacks α-ketoglutarate leading to decarboxylation and generation of an oxoferryl (Fe(IV)═O) species with bound succinate. The high spin Fe(IV)═O species has been trapped and characterized by Mössbauer spectroscopy.[74] The high-valent iron species then abstracts a hydrogen atom from taurine, which would generate a

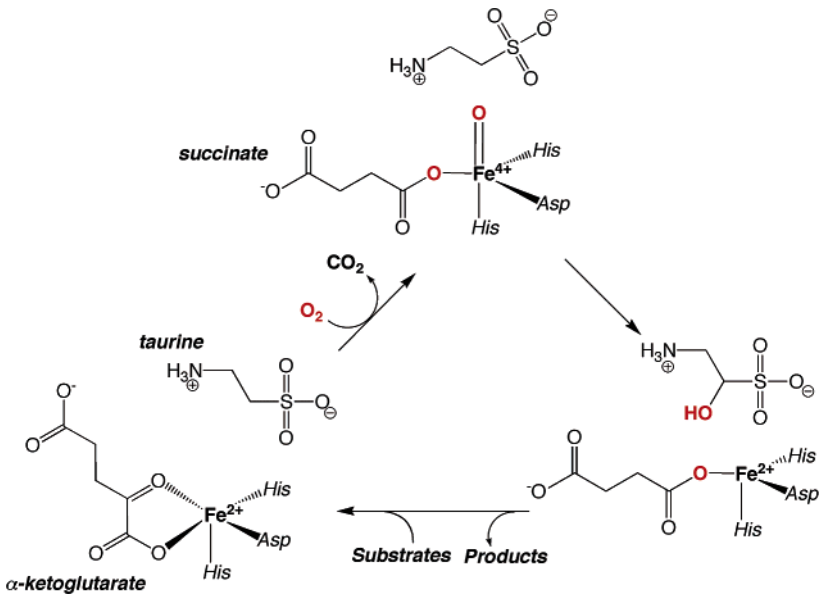

Figure 13. TauD reaction mechanism. The positions of the oxygen atoms from O_2 are shown in red. Redrawn from Price et al.[75]

substrate radical and hydroxy-Fe^{3+}, in a step that exhibits a deuterium isotope effect (k_H/k_D) of 35.[75] The next step is hydroxylation of the substrate radical likely through a radical rebound reaction to yield the product, hydroxytaurine. Release of succinate and hydroxytaurine return the enzyme to its active state for another round of catalysis. Given the complexity of the chemical steps, it seems surprising that the rate-limiting step is product release, as shown by solvent viscosity effects.[76]

2.2.2. Methane Monooxygenase (MMO): Carboxylate-Bridged, Diiron-Catalyzed Alkane Functionalization

A member of the bacterial multicomponent monooxygenase (BMM) family, MMO is a three-component system consisting of a hydroxylase that catalyzes oxidation of the substrate, a reductase that transfers electrons to the hydroxylase, and an auxiliary protein that enhances the activity and specificity of the hydroxylase. The metal scaffold plays a strategic role in the MMO-catalyzed oxidation of methane to methanol by offering a ligand environment that stabilizes a cluster of two irons in their high-valent states. This is important because it allows the generation of a stabilized high-valent oxo species in a different way than cytochrome P_{450}. In MMO, the two electrons required to stabilize the oxygen atom are supplied by the oxidation of 2 Fe(III) ions to 2 Fe(IV)s, while in P450, the first electron comes from oxidation of the heme Fe(III) to Fe(IV), and the second electron comes from oxidation of the porphyrin.

The role of the metal centers in catalyzing methane oxidation by methane monooxygenase (MMO) is interesting because this involves the cleavage of the C−H bond of methane with a 440 kJ/mol bond dissociation energy. Although such an uphill energy landscape would imply radical chemistry, there is active discussion about different proposed mechanisms, including whether the MMO-catalyzed oxygenation reaction proceeds through a cationic or radical pathway and whether different substrates operate through the same or discrete mechanisms, whether the hydrogen atom abstraction step is stepwise or concerted with substrate oxygenation, and whether the mechanism includes an iron−carbon bond. C−H bond activation in Nature is often catalyzed by metallocenters in monooxygenases. Although cleavage of the C−H bond is energetically difficult, the overall oxygenic conversion of methane to CO_2 (eq 1), is highly favorable. Because of its high energy density of 43.9 kJ/mol·g, methane is a widely used fuel. Methane oxidation supports the growth of methanotrophic bacteria, which can use methane as their only energy and carbon source.

$$CH_4 + 2O_2 \rightarrow CO_2 + 2H_2O \qquad \Delta G = -809.6\ \text{kJ/mol} \tag{1}$$

$$CH_4 + NADH + H^+ + O_2 \rightarrow CH_3OH + NAD^+ + H_2O \tag{2}$$

The BMM family includes other methane, alkane (propane), toluene, phenol, and ammonia monooxygenases. These enzymes catalyze the first steps in pathways that allow microbes to utilize alkanes, alkenes, aromatics, and ammonia as sources of energy and carbon or nitrogen for growth. There are two types of MMO, and structures are available for each: a soluble enzyme containing an oxygen-bridged diiron cluster[77,78] and a Cu-containing membrane bound enzyme.[79,80] The latter enzyme is expressed in all methanotrophs at elevated copper concentrations. Much less is known about the mechanism of the copper enzyme, so this review will focus on the diiron MMO.

As mentioned above, aspects of the MMO reaction cycle remain controversial. Figure 14 depicts some of these divergent views. There is evidence for an initial complex of $MMOH_{red}$ with O_2 (intermediate O),[81] two peroxy intermediates differing in protonation state (intermediates P* and P),[82,225] a reactive high-valent species (intermediate Q), a bound radical (intermediate R), and an enzyme−product complex (intermediate T).[83] These intermediates have been identified by elegant transient kinetics methods coupled to various forms of spectroscopy. Excellent reviews are available describing the overall mechanism[77,84,85] and the part of the cycle involving the reaction with the substrate.[84] The first part of the catalytic cycle, which involves generation of the active oxygenating state of the diiron catalytic center, includes intermediates H_{ox}, H_{red}, P*, P, and Q. This review will concentrate mainly on the steps involving intermediates

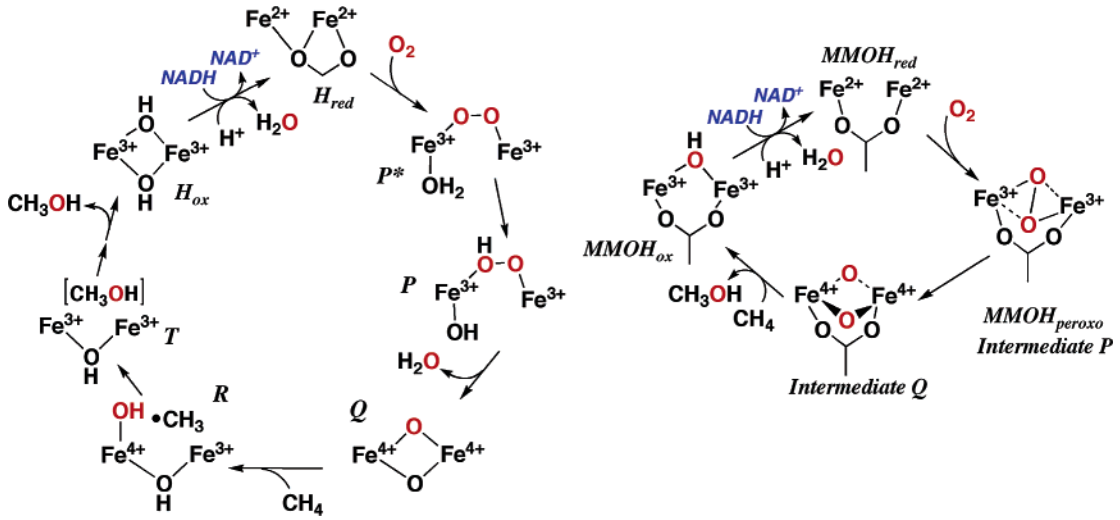

Figure 14. Reaction cycle of MMO. Left panel: modified from ref 90. Right panel: modified from Baik et al.[84] The positions of the oxygens from O_2 are shown in red.

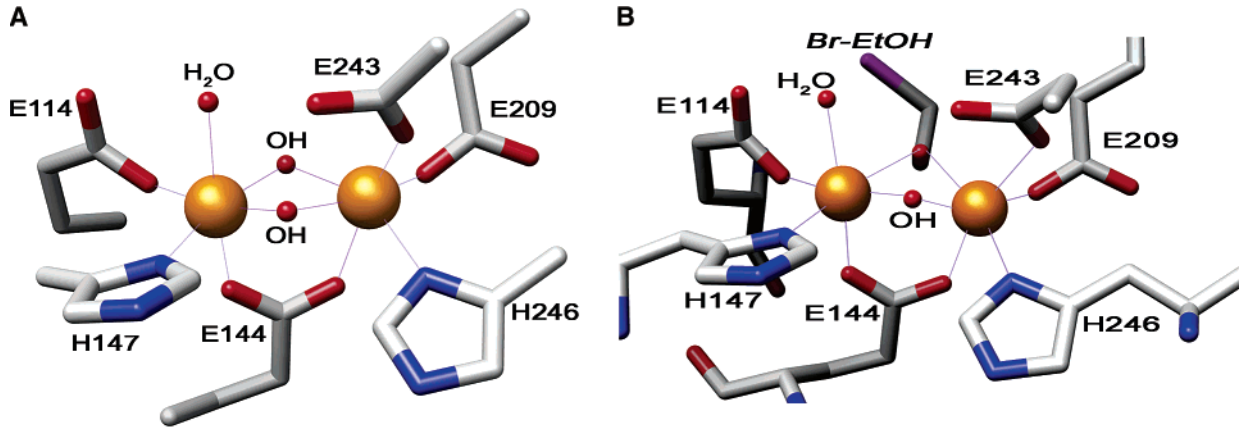

Figure 15. (A) Diferric MMOH ($MMOH_{ox}$), from 1.7 Å structure, PDB no. 1MTY.[91] (B) Diferric MMOH ($MMOH_{ox}$) with bound bromoethanol, from 1.96 Å structure, PDB no. 1XVG.[92]

Q and R, because the focus of this review is on the role of the metal in promoting catalysis.

The soluble diiron MMO has a wide substrate specificity, including various alkanes, halogenated alkane (trichloroethylene, chloroform, dichloromethane, dichloroethane, trichloroethane) and aromatic compounds, and heterocyclic organics; thus, there is industrial interest in the use of MMO to catalyze oxygen incorporation into fine chemicals that are difficult to oxidize and in cleanup of halogenated xenobiotics. The soluble MMO contains three components: the MMO hydroxylase (MMOH), a 245 kDa hexameric protein with an $\alpha_2\beta_2\gamma_2$ structure, which binds and oxidizes the substrate; MMOR, a 38 kDa NADH-dependent reductase that reduces MMOH; and MMOB, a 16 kDa auxiliary protein that enhances the activity and specificity of MMOH. The structures of MMOH, MMOB,[86,87] and of two domains of MMOR[88,89] are known. MMOH contains an active site diiron center, which in the resting oxidized state is a carboxylate-bridged diferric center located within a four-helix bundle (Figure 15A). Also shown is the structure of a product-like complex in which one of the ligands is bromoethanol (Figure 15B), which was soaked into the crystal.

The key intermediate in the MMO reaction is intermediate Q, which has a diamond core structure consisting of two symmetric high-valent Fe(IV) ions bridged by the two oxygen atoms derived from O_2.[93] Intermediate Q incorporates 1 mol of oxygen from the diamond core center into methane to generate methanol. An important question is how methane functionalization occurs. One possibility is that it occurs by a radical rebound mechanism,[77,94] analogous to that first proposed by Groves for cytochrome P_{450},[95] in which H-atom abstraction by an activated Fe−oxo complex generates a methyl radical and a cluster-bound hydroxy radical that recombine (rebound) to form methanol. Another possibility is direct oxygen insertion into a C−H bond. Measurement of deuterium kinetic isotope effects for the overall MMO reaction of between 23 and 50 that are well above the classical limits of 7.0 provide support for rate-limiting hydrogen atom abstraction in a radical mechanism involving hydrogen tunneling.[96,97] Also, MMO-catalyzed oxidation of chiral 1-[^{2}H,^{3}H]-ethane was shown to result in extensive racemization, consistent with an intermediate likely to be a radical.[98,226] The activation energy for substrate hydroxylation, which reflects predominantly the rate-limiting H-atom abstraction from methane by intermediate Q, was calculated to be 77.7 kJ/mol.[99] Analyses of the reaction of intermediate Q with various substrates demonstrated that, with a few (methane, acetonitrile) substrates, H-atom abstraction is rate-limiting, while for most (ethane, methanol), the rate-limiting step is substrate binding.[100] The above analyses strongly support hydrogen atom abstraction to generate a methyl radical as an intermediate. Radical spin trap experiments have also been interpreted to demonstrate radical intermediates in the MMO mechanism.[101,102]

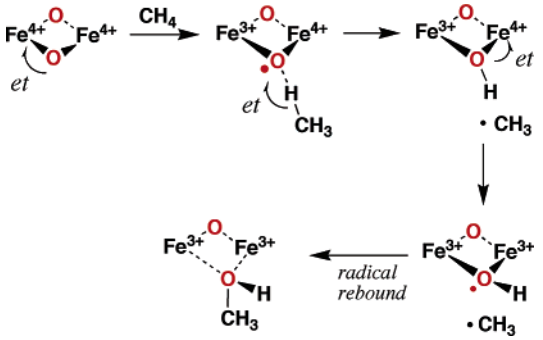

Figure 16. Radical rebound in the MMO mechanism. Based on Baik et al.[84]

A review of experiments using mechanistic probes, so-called radical clock substrate probes, to address the involvement of radical or cationic intermediates is available.[84] These probes rearrange in a manner that would imply the type of intermediate, and measurements of the rates of the rearrangement reaction provide lifetimes for the intermediate. Regarding the evidence for cationic intermediates, Baik et al. state that it is indisputable that cationic rearrangement products are obtained in MMO hydroxylations (for example, generation of homocubanol from methylcubane); however, because small amounts of these products are observed and because often both cationic and radical rearrangement products are observed, "there is not a consensus as to the mechanistic interpretation of these results".[84] On the other hand, on the basis of radical clock experiments with a series of methylcyclopropanes with different lifetimes in solution, it was concluded that whether an intermediate rearranges depends on steric effects.[103] It was proposed that intermediates with little bulk near the site of hydrogen atom abstraction are quenched or react with the diiron center before they can rearrange (even for "fast probes"), while intermediates with bulky substituents near the C−H bond yield reasonable amounts of rearrangement products.[103]

Consistent with the results described above, computational methods also suggest a radical mechanism involving H-atom abstraction (Figure 16).[84] Beginning at the step at which intermediate Q reacts with substrate, the reaction is proposed to involve nucleophilic attack of methane on one of the bridging oxo groups in "Q" followed by proton-coupled electron transfer from the bridging oxo group to one of the Fe(IV) atoms. This process would form a methyl radical, which has been suggested to be a "bound radical".[84] Electron transfer to the Fe^{4+} site would lead to a hydroxy radical that would recombine with the methyl radical to generate methanol.

2.2.3. Heme Oxygenase

This section will discuss the use of heme both as a substrate and a catalyst to catalyze a reaction that is both sterically and chemically difficult: the conversion of heme to biliverdin, CO, and iron (Figure 17). Several recent reviews on the physiology[104,105] and mechanism[106−109] of heme oxygenase (HO) are available. This enzyme plays an important role in heme and iron homeostasis and is present in nearly all classes of eukaryotes and bacteria. In cyanobacteria, algae, and plants, HO is involved in generating the chromophores for photosynthesis.[110,111] There are two forms of mammalian HO (HO1 and HO2), which share similar physical and kinetic properties but exhibit different physiological roles and organ locations. The HO oxygenation reaction is coupled to two other enzymes: cytochrome P_{450} reductase, which provides the required reducing equivalents, and biliverdin reductase, which converts the unstable green product biliverdin to yellow bilirubin.

The reaction catalyzed by HO occurs with absolute regiospecificity—the mammalian HO1 or HO2 cleaves heme to excise only the α-meso carbon (bold lines in Figure 17), while some bacterial HOs cleave the tetrapyrrole ring at the *β* position.[112] The oxygenation catalyst is the hydroperoxyheme,[113] instead of compound **I** (an oxyferryl coupled to a radical), which is an intermediate in P_{450} and other oxygenases. Stabilizing the hydroperoxy ferric intermediate and directing the reactive oxygen specifically to only one of the four electronically equivalent meso carbon atoms requires exquisite tuning of the electronic and steric environment by the active site scaffold of HO. This scaffold includes the porphyrin ring and its various appendages as well as important active site residues that control the orientation of the heme at the active site and control the reaction trajectory.

The substrates and products of the HO reaction have important regulatory and metabolic roles. Heme is the prosthetic group of many electron-transfer proteins and redox enzymes. Heme also regulates the expression of genes involved in oxygen utilization in prokaryotes[114] and in higher eukaryotes.[115,116] Iron is present in heme and many non-heme metalloenzymes and serves as an effector for transcriptional regulatory proteins.[117,118] Bilirubin is an antioxidant,[119] and biliverdin reductase has been shown to have multiple roles in gene regulation and in metabolic signaling.[105] Finally, CO serves as a signaling molecule that activates guanylate

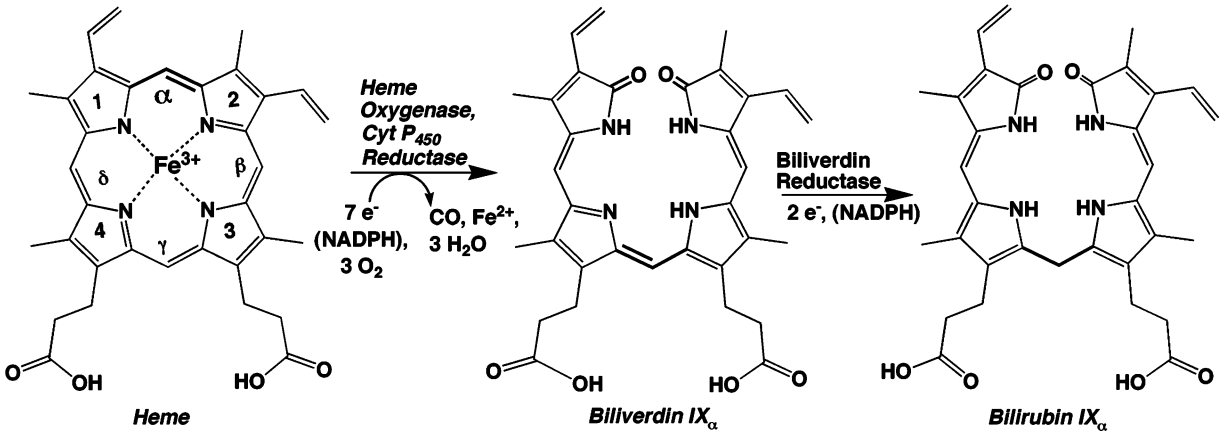

Figure 17. The HO reaction coupled to P450 reductase and biliverdin reductase.

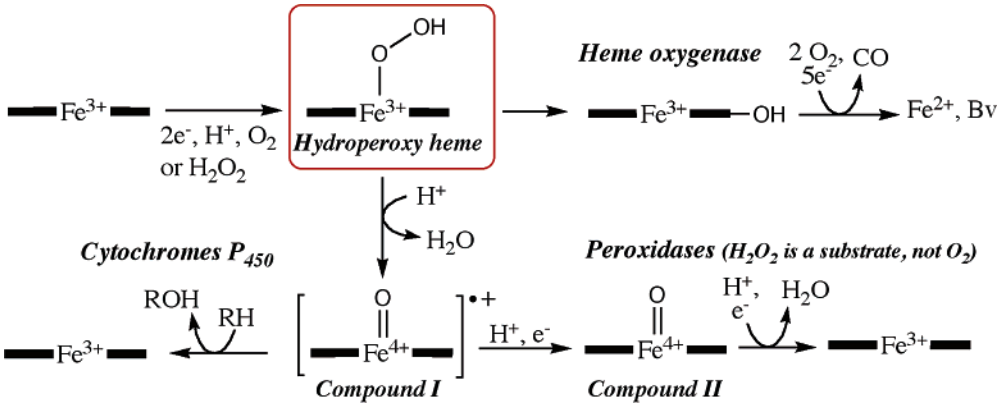

Figure 18. Oxygenating species in the oxidases. Cytochromes P_{450} and heme oxygenase use O_2 as their natural substrate, while peroxidases uses H_2O_2, though H_2O_2 can supplant the requirement for O_2/electrons via a peroxide shunt.

cyclase.[120] CO also appears to be involved in regulating circulating blood oxygen levels.[121]

Like cytochrome P_{450} or MMO, HO catalyzes substrate hydroxylation, but through quite a different mechanism that utilizes a different hydroxylating agent (Figure 18). The HO-catalyzed reaction[108] requires seven electrons that are transferred in several cycles of NADPH-dependent reduction with NADPH:cytochrome P_{450} reductase and three successive O_2-dependent oxygenation steps (Figure 19A), and HO must coordinate all these reactions without misfiring. The first oxygenation (Figure 19B) leads to hydroxylation of the porphyrin α-meso carbon to yield the α-*meso*-hydroxyheme. The second converts the hydroxyheme to verdoheme (Figure 19C), while the third oxygenation reaction converts verdoheme to ferric biliverdin (not shown in detail), which upon one-electron reduction releases iron in the ferrous state to form biliverdin.

In the first oxygenation reaction, NADPH:cytochrome P_{450} reductase transfers one reducing equivalent to convert the ferric heme to the ferrous state (species **1**, Figure 19A), enabling O_2 binding. Transfer of a proton and a second electron generates an Fe^{3+}-hydroperoxo species, which chemical and resonance Raman studies have shown is the active oxygenation agent in HO.[106,122,123] This hydroperoxy ferric oxygenation agent is distinct from compound **I** (an oxy ferryl porphyrin coupled to a protein or porphyrin radical) of cytochrome P_{450} (see Figure 18). Compound **I** has been ruled out as in intermediate in heme metabolism based on the inability of alkyl peroxides and peracids to replace oxygen and electrons in formation of the hydroxyheme.[124] Furthermore, it was recently shown that compound **I**, when generated in HO, is unable to hydroxylate the heme.[125] There have been a number of investigations aimed at understanding how HO stabilizes the hydroxyperoxy heme and prevents formation of compound **I**. In P_{450}, the heme iron contains a cysteine residue as a proximal ligand. This provides a strong electronic "push effect" of the thiolate ligand to help activate the Fe(II)−O_2. In HO, the proximal heme ligand is histidine, which is a much weaker electron donor than cysteine, providing a lesser degree of "push" (see Fujii et al.[126] for details). Another difference between the HO and P_{450} systems relates to their hydrogen relay systems, which play key roles in their hydroxylation mechanisms. Cytochromes P_{450} contain a highly conserved proton relay system (Thr and Asp) on the distal side of the heme, which provides protons to activate Fe(II)-bound O_2, to facilitate protonation of the hydroperoxo iron at the distal oxygen leading to formation of the reactive high-valent compound **I**. On the other hand, for HO, instead of facilitating O−O bond cleavage and elimination of hydroxide or water, there is a H-bond network near the α-meso edge of the heme that consists of a water molecule (depicted in Figure 19B) H-bonded to a conserved essential Asp (D140, not shown) that is proposed to stabilize the bound hydroperoxide and to facilitate oxidization of the α-meso carbon by the terminal oxygen of the bound hydroperoxide (Figure 19B).[127,128] Thus, apparently, in HO, delivery of the second proton to the terminal oxygen of the Fe−OOH is disfavored, such that only a hydrogen bond is formed. Disruption of this network by mutation of any of the involved residues leading to formation of the oxyferryl species and to the unleashing of peroxidase activity is one of several results that support the importance of this network in the HO mechanism.[109,129] In HO, a helix is located in the distal pocket of the heme (Figure 20), and two glycine residues, located near the heme pocket (one of these is shown in Figure 19B), would be unable to facilitate O−O bond cleavage as the proton relay system does in P_{450}. In summary, there are subtle changes in hydrogen bonding and proton transfer that lead to heme oxygenation in HO versus compound **I** formation in P_{450}.

Since there are four meso carbons, how does HO catalyze the selective oxidation at the α-meso position? One issue is stereochemistry. In the recent 1.9-Å structure of HO with azide (an O_2 analogue) coordinated to the iron of heme, the azide stretches across the heme plane with its terminal N directed toward and only 3.4 Å from the α-meso carbon (Figure 20).[130] Most of the heme atoms are covered by a helix (the distal F helix); however, the α-meso carbon is relatively exposed. These results suggest the mechanism shown in Figure 19B, where a combination of steric constraints and H-bonding interactions orient the terminal oxygen atom of the hydroperoxo heme intermediate near the α-meso carbon. Then, as shown in Figure 19, the meso hydroxylation appears to involve electrophilic addition of the terminal oxygen of the Fe−OOH group to the double bond of the porphyrin to give a cationic intermediate, followed by loss of a proton to rearomatize the porphyrin ring.

The next two reactions are much less understood. The second is reaction of the hydroxy-heme with another mole of O_2 to generate verdoheme (species **3**) and CO (Figure 19C). This subreaction is coupled to the uptake of one electron and appears to occur through an Fe^{2+} peroxy radical intermediate as shown.[106] O−O bond cleavage is proposed to lead to an oxy radical and a ferryl species that rearranges

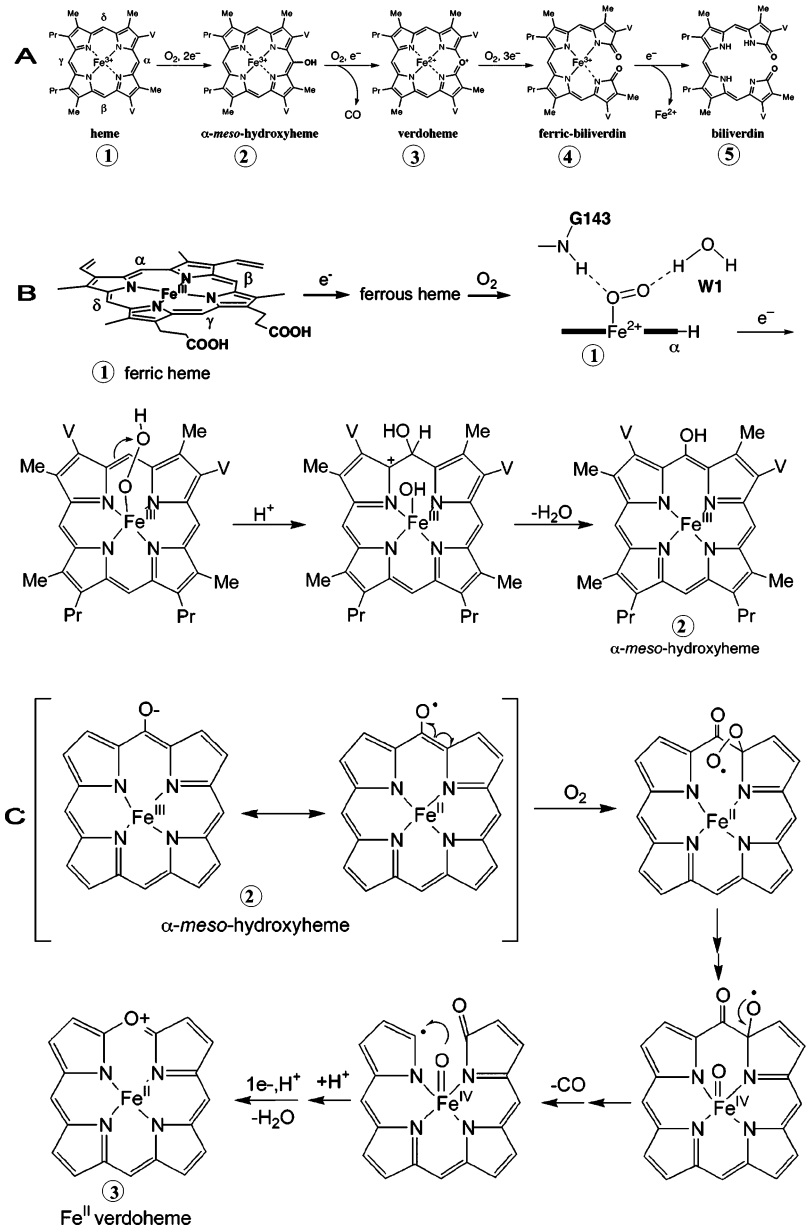

Figure 19. Proposed mechanism of HO. (A) Formation of α-meso hydroxyheme. Reprinted with permission from ref 109. Copyright 2003, Academic Press, Elsevier. The three oxygenation steps in the HO-catalyzed reaction. Reprinted with permission from ref 131. Copyright 2005 American Society for Biochemistry and Molecular Biology. (B) The initial steps in the HO mechanism leading to OH-heme formation. Redrawn from refs 106 and 133. Orientation of the O_2 above the α-meso carbon of the tetrapyrrole based on the structure of the azide adduct.[130] (C) Conversion of hydroxyheme to verdoheme.

to a carbonyl radical, which eliminates as CO.[106] CO release would generate a porphyrin radical that could undergo protonation and one-electron uptake to form verdoheme. According to this mechanism, although there are a number of proposed radical interconversions, this last step is the only one that involves electron uptake.

The oxygenation of verdoheme to ferric biliverdin involves uptake of four electrons and O_2 to generate Fe^{2+}, which is released, and biliverdin. These reactions have been extensively discussed, and alternative mechanisms have been proposed by Matsi et al.[131] and Colas and Ortiz de Montellano.[106]

Surprisingly, given all the complex redox and oxygenation chemistry, the rate-limiting step in the HO mechanism is release of biliverdin.[132] However, biliverdin reductase markedly stimulates biliverdin release so that in vivo the slow step appears to be conversion of verdoheme (species **3**) to

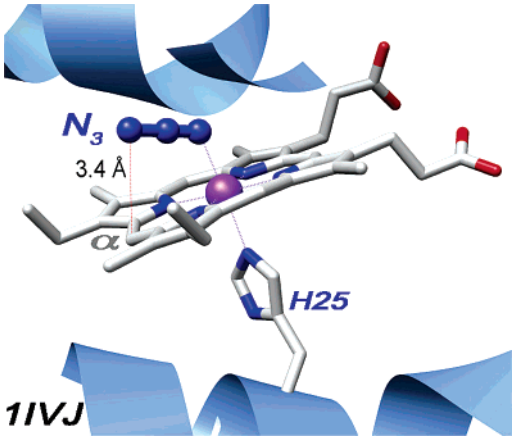

Figure 20. Structure of the heme−azide adduct of HO1. Drawn from PDB no. 1IVJ using Chimera.

ferric biliverdin (species **4**).[132] Biliverdin reductase couples to the HO reaction to reduce the C10 γ bridge of biliverdin to generate bilirubin.

2.3. Low-Valent Metal Sites in Enzymes To Catalyze Difficult Reactions

While methane oxidation using O_2 as an electron acceptor is highly exergonic ($\Delta G = -809.6$ kJ/mol, section 2.2.2.), many microbes live much nearer the thermodynamic equilibrium by coupling the oxidation of H_2 to the reduction of CO_2 to methane (eq 3) or acetic acid (eq 4). Although anaerobes also can make use of more thermodynamically favorable oxidants such as sulfate or nitrate, it is this more difficult chemical equilibrium expressed in eqs 3 and 4 that will be the focus of the remainder of this review. Although methanogenesis and acetogenesis are much less energetically favorable, these anaerobic processes are key components of the global carbon cycle. The lifestyle of a class of archaea called methanogens is responsible for the generation of 560 million metric tons of methane every year. Despite the difference in energetics, sufficient methanogenesis occurs to leave a slight surplus of methane in our atmosphere (1.7 ppm), whose rising concentration has been a source of concern, since methane is a potent greenhouse gas.

The enzymes that will be covered (methyl-CoM reductase, CO dehydrogenase/acetyl-CoA synthase, and cobalamin-dependent methyltransferases) are interesting not only because they make the "life at the edge" scenario feasible, but also because the enzymes are amazing examples of unusual metallobiochemistry to catalyze difficult reactions.

$$H^+ + HCO_3^- + 4H_2 \rightarrow CH_4 + 3H_2O \qquad \Delta G^{\circ\prime} = -135.6 \text{ kJ/mol} \quad (3)$$

$$2HCO_3^- + 4H_2 \rightarrow CH_3COO^- + 4H_2O \qquad \Delta G^{\circ\prime} = -104.6 \text{ kcal/mol} \quad (4)$$

2.3.1. Methyl-Coenzyme M Reductase (MCR): A Low-Valent Nickel Tetrapyrrole for Methane Synthesis and Anaerobic Methane Oxidation

All biologically produced methane is formed as a result of the methyl-coenzyme M reductase (MCR)-catalyzed conversion of methyl-coenzyme M (methyl-SCoM) and *N*-7-mercaptoheptanoylthreonine phosphate (CoBSH) to methane and the CoB-S-S-CoM heterodisulfide (eq 5).[134] CoBSH serves as the electron donor[135] and has been proposed to also be the proton donor[136] for this reaction. At the heart of MCR is a nickel hydrocorphin called Coenzyme F_{430} (Figure 21),[137−139] which is located at the base of a narrow hydrophobic well that accommodates the two substrates and shields the reaction from solvent.[140] Unlike heme, which is fully conjugated, F_{430} only contains five double bonds and is the most reduced tetrapyrrole in Nature.

$$\text{Methyl-SCoM} + \text{CoBSH} \rightarrow CH_4 + \text{CoB-S-S-CoM} \quad (5)$$

The active state of MCR is called MCR_{red1}, which contains low-valent Ni(I).[136,143,144] The X-ray crystal structures of the inactive nickel(II) enzyme in complex with CoM and CoB ($MCR_{ox1-silent}$) and in complex with the heterodisulfide CoM-S-S-CoB product (MCR_{silent}) have been resolved at 1.16 and 1.8 Å resolution, respectively.[145] MCR contains three nonidentical subunits in an $(\alpha\beta\gamma)_2$ structure that is predominantly composed of helices and forms an overall ellipsoidal shape

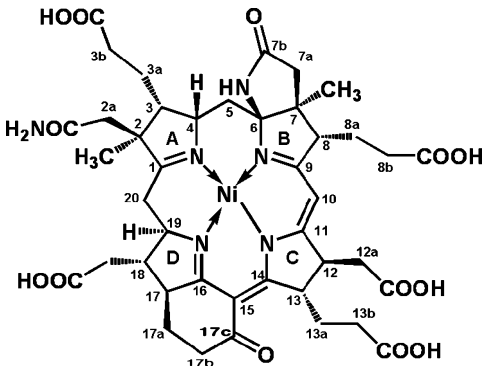

Figure 21. Structure of the nickel tetrahydrocorphinoiod Coenzyme F_{430} based on X-ray and NMR methods.[141,142]

of about 120 × 85 × 80 Å. Because of the low redox potential of the Ni(II)/(I) couple, great care must be taken to isolate the enzyme in the Ni(I) oxidation state; otherwise, it contains inactive Ni(II) and is bright yellow. The Ni(I) state of the cofactor is green and paramagnetic, exhibiting the fairly typical EPR spectra of a d^9 system with $g_{||}$ (2.2−2.3) > g_{perp} (2.05) > g_e (2.0),[146] where the "parallel" and "perpendicular" subscripts designate the symmetry of the EPR signals (the subscript "e" is the free electron *g*-value). On the basis of the ^{61}Ni and ^{14}N hyperfine coupling values obtained by ENDOR and EPR studies,[147] it is estimated that approximately 80−90% of the unpaired spin density is on nickel in the MCR_{red1} state. The many spectroscopic studies of MCR that have been performed, including EPR, ENDOR, X-ray absorption, and resonance Raman, have been summarized.[144,148] MCD[149,150] and advanced EPR[151] studies not included in those reviews have been recently described.

Methane formation by MCR occurs with a turnover number of over 100 s^{-1} and with a relatively high value of k_{cat}/K_m (methyl-SCoM) of ~1 × 10^5 $M^{-1}s^{-1}$.[152,153] Two general types of mechanisms have been considered for the MCR-catalyzed reaction: one involving an organometallic methyl-Ni intermediate (Figure 22A) and another that involves a methyl radical and hydrogen abstraction from CoBSH (Figure 22B). In mechanism I, MCR binds both substrates (Step 1) and catalyzes an S_N2-type displacement of the methyl group of methyl-CoM to form a methyl-Ni(III) intermediate (Step 2). Methyl-Ni(III) is a highly oxidizing species and, in Step 3, accepts an electron from CoB-S^- to generate a thiyl radical on CoM and methyl-Ni(II). In Step 4, protonolysis of the methyl-Ni species generates methane and Ni(II), while a bond between CoB and the CoM radical forms a highly reducing disulfide radical anion. Electron transfer from the radical anion to Ni(II) yields the CoM-S-S-CoB heterodisulfide and regenerates the active Ni(I) form of MCR (Step 5).

The experimental support for this mechanism includes model studies of the reaction between the Ni(I) form of the pentamethyl ester of F_{430} and activated methyl donors (e.g., methyl sulfonium ions and methyl iodide) to yield methane through protonation of a methylnickel intermediate.[155−157] Furthermore, reaction of the Ni(I) state of F_{430} and a thiyl radical with a methyl thioether yields methane and the corresponding disulfide.[158]

Figure 22B describes a proposed mechanism, based on computational studies, that avoids the methyl-Ni species.[159] *Step 1* involves cleavage of the C−S bond of methyl-CoM to generate a methyl radical and a thiyl radical on CoM. The Ni(I), in this case, is proposed to donate an electron to

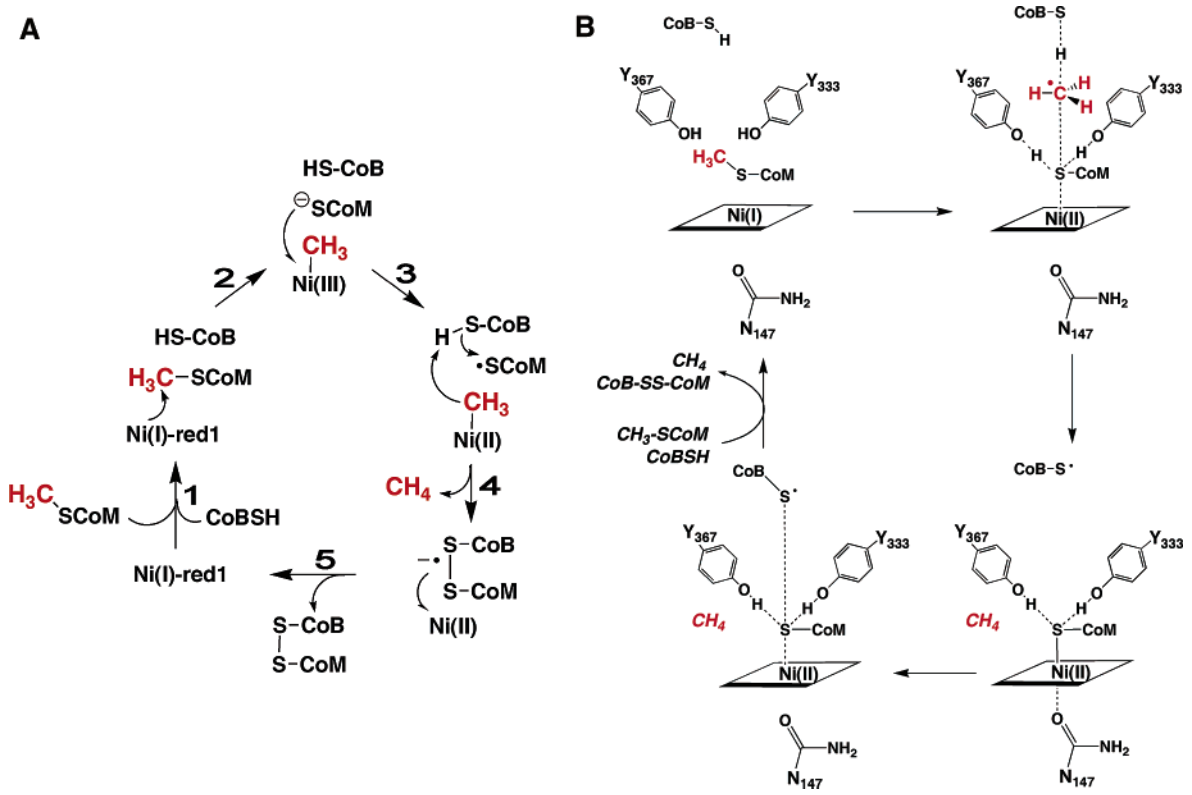

Figure 22. (A) MCR mechanism I involving a methyl-Ni and disulfide anion radical. (B) MCR mechanism involving a methyl radical and H-atom abstraction from CoB. Redrawn based on Siegbahn.[154]

the incipient thiyl radical, generating the CoM-S$^-$ anion, which would gain stabilization by coordination to Ni(II). Hydrogen bonding interactions from two active site tyrosine residues are proposed to neutralize and stabilize the negative charge on the CoM thiolate once the methyl radical is formed. In this mechanism, the major role of the Ni is to facilitate C−S bond cleavage by a redox process and to stabilize the product of C−S homolytic bond cleavage by forming a coordination complex with the sulfur of CoM. In *Step 2*, the methyl radical is proposed to abstract a H-atom from CoBSH to form methane and a thiyl radical on CoB. *Step 3* involves formation of a disulfide anion radical between CoBS• and CoMS$^-$. Finally, reduction of Ni(II) by the anion radical regenerates the active Ni(I) state, and products are released.

Distinction between the two mechanisms will require characterization of the intermediates in the MCR reaction, which so far have not yielded to spectroscopic identification. Future studies aimed at observing these intermediates would likely need to take advantage of substrate analogues and/or variant forms of MCR that exhibit altered rates for catalyzing intermediate steps in the reaction cycle. Another important area of future study is determination of the crystal structure of the highly labile active Ni(I) or perhaps an alkyl-Ni intermediate.

2.3.2. CO Dehydrogenase/Acetyl-CoA Synthase

CO dehydrogenase/acetyl-CoA synthase (CODH/ACS) enables acetogenic microbes to grow using H_2 as an electron donor and CO_2 as an electron acceptor and source of carbon (reaction 4). It also allows microbes to use carbon monoxide as their sole source of carbon and energy. Microbial CO metabolism is globally important, since 10^8 tons of CO are removed from the lower atmosphere of the earth by bacterial

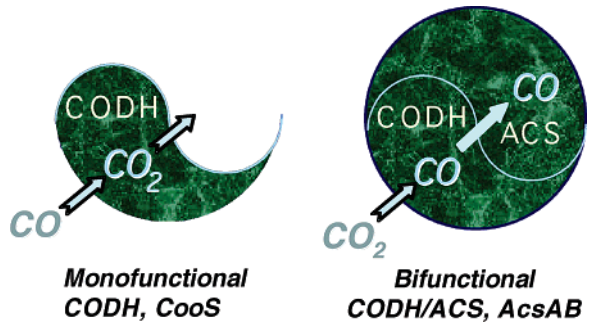

Figure 23. Cartoon of the monofunctional CODH and the bifunctional CODH/ACS.

oxidation every year,[160] helping to maintain ambient CO below toxic levels. There are three varieties of CODH: the monofunctional molybdopterin copper iron−sulfur CODH, the monofunctional nickel iron−sulfur CODH, and the bifunctional CODH/ACS (containing three discrete Ni sites). Although the monofunctional CODH and the CODH associated with the CODH/ACS complex have the same catalytic centers and similar overall structures, they are separate gene products, are regulated differently, and differ in their catalytic bias (Figure 23). The monofunctional CODHs function to bind CO with high affinity and oxidize it rapidly to CO_2, while the role of the CODHs associated with the CODH/ACS complex is to reduce CO_2 to CO and channel this CO to the ACS active site. A review describing CO metabolism and the properties of these enzymes is available.[161]

CODH is a redox-chemical transformer that generates high-energy electrons as it catalyzes CO oxidation to CO_2 (eq 6). The CO_2 is then fixed into cellular carbon by one of the reductive CO_2 fixation pathways, like the Calvin−Benson−Bassham Cycle, the reverse TCA cycle, the 3-hydroxypropionate cycle, or the Wood−Ljungdahl pathway.

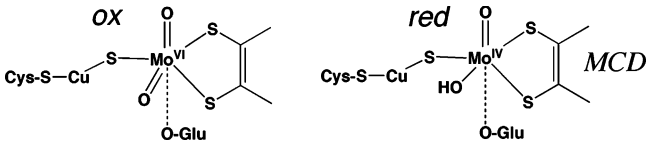

Figure 24. Cu−Mo center in the molybdopterin CODH.

The turnover number for CO oxidation to CO_2 by one of the CODHs reaches 40 000 s^{-1} with a catalytic efficiency reaching the diffusion-controlled range of 2×10^9 M^{-1} s^{-1}.[162] As a reductant, CO is approximately 1000-times more potent than NADH.

Coupling CODH to ACS forms a machine that catalyzes formation of acetyl-CoA from CO_2, a methyl group, and CoA. In this case, CODH facilitates the scaling of a formidable free energy barrier in catalyzing the reverse reaction − reduction of CO_2 to CO (eq 6). Then, ACS catalyzes the formation of a C−C and a C−S bond by the ligation of CO to a methyl group and to the thiol group of Coenzyme A to form acetyl-CoA (eq 7). The methyl group is donated by an organometallic methylcobamide (a vitamin B_{12} derivative) species on a protein called the corrinoid iron−sulfur protein (CFeSP), which is described in more detail in the following section. Formation of acetyl-CoA is a prodigious reaction from a bioenergetic perspective ($\Delta G^{\circ\prime} = -32$ kJ/mol) because cells couple cleavage of the thioester bond to ATP formation. From the viewpoint of cellular economy, the acetyl-CoA can serve as a metabolic building block that is an entry point into many biochemical pathways.

$$2\ \text{electrons} + 2H^+ + CO_2 \leftrightarrow CO + H_2O \qquad \Delta E^{\circ\prime} = -558\ \text{mV}^{163} \quad (6)$$

$$CO + CH_3\text{-CFeSP} + \text{CoA} \rightarrow \text{acetyl-CoA} + \text{CFeSP} + H^+ \quad (7)$$

2.3.2.1. CO Dehydrogenase: A Catalytic Nickel Iron Sulfur Cluster and a Redox Wire. The molybdopterin Cu CODH consists of an $(\alpha\beta\gamma)_2$ structure with a molecular mass of ∼250 kDa,[164] and its structure has been determined.[165,166] The active site contains a Cu linked to a Mo-pterin, molybdopterin cytosine dinucleotide (MCD), and CO is proposed to bind the Cu (Figure 24).[165] These CODHs also contain 2 mol of FAD and 8 Fe and 8 acid-labile sulfide, which are present as [2Fe−2S] centers[167] and are involved in electron transfer to the catalytic Cu−Mo-pterin center.[168]

The Ni CODH is a fairly well-studied enzyme. On the basis of the X-ray crystal structures of two monofunctional CODHs (encoded by the *cooS* gene) and one CODH from the CODH/ACS structure, the enzyme is a mushroom-shaped homodimer containing five metal clusters (clusters B, C, and D).[169−172] The C-cluster is a [3Fe−4S] cluster bridged to a heterobinuclear NiFe cluster and is the catalytic site for CO oxidation (Figure 25). Clusters B and D are $[4Fe-4S]^{2+/1+}$ clusters that transfer electrons between the C-cluster and external redox proteins.

The CODH reaction requires the delivery of CO and water to the active site. Two channels converge just above the Ni site: a hydrophobic channel that is proposed to deliver CO to the active site and a solvent channel that is proposed to deliver the other substrate, water. This is a ping-pong reaction: CODH is reduced by CO in the "Ping" step (Steps 1−4, Figure 26) and the reduced enzyme transfers electrons

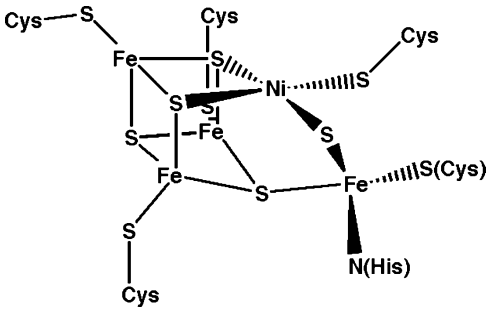

Figure 25. Cluster C of CODH. From PDB no. 1OAO.

to an external redox mediator like ferredoxin in the "Pong" step (Step 5).

Step 1 of the reaction involves binding of CO and water to cluster C (Figure 26). The proposal that an open coordination site above Ni in the C-cluster is the site of CO binding[169,171] is supported by Fourier transfer infrared (FTIR) studies of CO binding to the *Moorella thermoacetica* CODH, which revealed several IR bands that were attributed to a Ni−CO complex in the C-cluster.[173] ^{17}O-ENDOR studies indicate that hydroxide binds to the Fe site (called Ferrous component II) that is bridged to Ni.[174] Binding of water to iron would be expected to lower its pK_a, which would facilitate formation of an active hydroxide, as in carbonic anhydrase.[175] Furthermore, there are several basic residues ("Base" in the figure = Lys563, His113) near the C-cluster that have been proposed to participate in these acid−base reactions.[169,171] Accordingly, mutagenesis of Lys587 and His113 *(M. thermoacetica* numbering) abolishes catalysis.[176]

In Step 2, the active metal-hydroxide is proposed to attack the M−CO complex to form a Ni−carboxyl complex. There is tentative IR evidence for a metal carboxylate intermediate.[173]

In Step 3, CO_2 is generated and released, a proton is eliminated, and cluster C undergoes two-electron reduction. The catalytic bases suggested to be involved in Step 1 could also participate in this reaction. The two-electron reduction should generate a transient Ni^0 state of the cluster as proposed by Lindahl;[177] however, with so many redox-active metal centers near the Ni, it seems unlikely that Ni^0 would exist for long. Figure 26 shows cluster C_{red2} resonating among several redox forms. Freeze-quench EPR studies show that when CODH in its resting C_{red1} state is reacted with CO, it converts rapidly (2×10^8 M^{-1} s^{-1}) to the C_{red2} state, before electrons are transferred to the chain of redox centers (clusters B and D).[178,179]

In Step 4, electrons are transferred from cluster C into the redox chain, which would return cluster C to its resting form and leave clusters B and D in a reduced state. The three clusters are approximately 10 Å apart, which is an ideal distance for rapid electron transfer.[180] Rapid kinetic studies have followed this internal electron-transfer reaction and shown that, at high CO concentrations, electron transfer can become rate-limiting.[179]

Step 5 constitutes the Pong step in which electrons are transferred from the reduced [4Fe−4S] clusters on CODH to the external mediators, for example, ferredoxin or other carriers. At high CO concentrations, Step 5 becomes rate-limiting.[178,179]

This reaction sequence shares similarity to the water−gas shift reaction (Figure 27), especially in the role of the metal centers to form coordination complexes with the various substrates and products of the reaction. Common

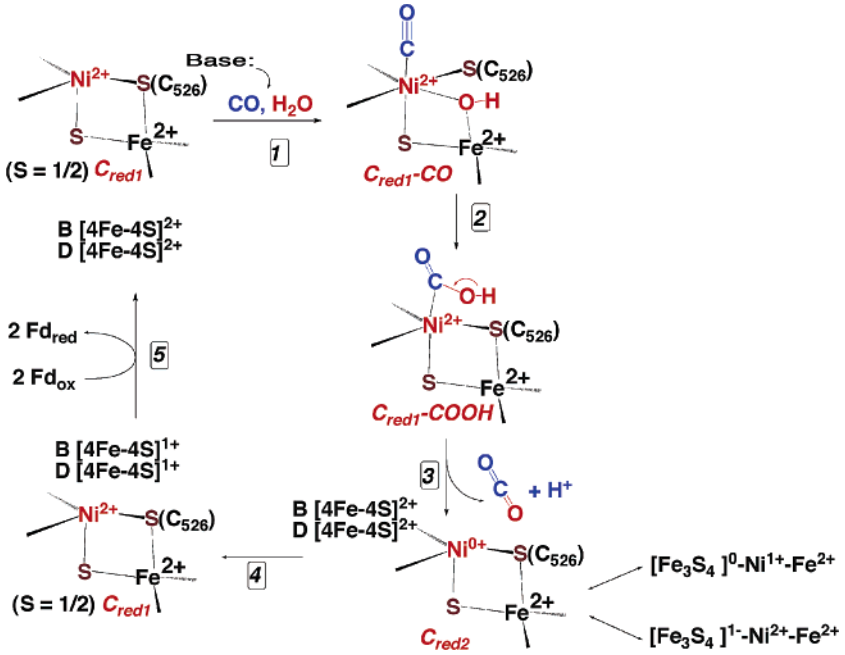

Figure 26. CODH mechanism.

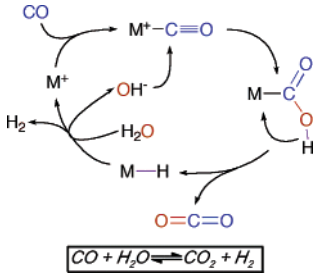

Figure 27. Water−Gas shift reaction.

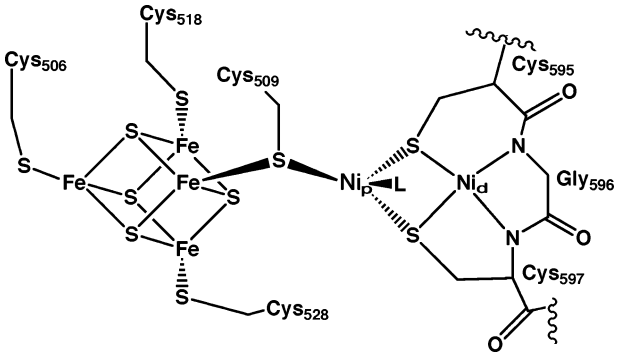

Figure 28. Structure of cluster A of ACS.

intermediates in the two reactions include a metal-bound carbonyl, a metal-bound hydroxide ion, and a metal carboxylate formed by attack of the M−OH on M−CO. A possible difference is that, in the water−gas reaction, elimination of CO_2 leaves a metal-hydride, whereas, in CODH, the metal center accommodates the two-electrons and a proton is released. However, it is perhaps premature to rule out metal-hydride intermediates, since CODHs have a weak CO-dependent hydrogen evolution.[181−183] On the other hand, it is clear that, unlike the water−gas shift reaction, H_2 is a minor product in the CODH-catalyzed reaction where very rapid electron transfer out of the active site is predominant. The proximity of a redox wire to rapidly oxidize the catalytic center is reminiscent of PFOR (section 2.1.2.). This strategy allows flexibility so that CODH is able to transfer electrons to various acceptors, and when the cell requires H_2, CODH can couple through a ferredoxin to a devoted hydrogenase.

2.3.2.2. Acetyl-CoA Synthase. Acetyl-CoA Synthase (ACS), encoded by the *acsB* gene, is part of the catalytic machine that converts CO_2, CoA, and a methyl group to acetyl-CoA. The other component of this machine is CODH, which is encoded by the *acsA* gene and is highly homologous to the monofunctional CODH (CooS) just described. Thus, as described in the cartoon in Figure 23, the substrate for ACS is produced by the adjacent CODH subunit, which reduces CO_2 to CO by a reversal of the mechanism shown in Figure 26. While a hydrophobic channel in the monofunctional CODHs aids in diffusion of CO from solution to the catalytic cluster C, for those CODHs that are part of the CODH/ACS machine, this channel appears to be absent. Instead, both CODH and ACS contain internal channels that interlink to form a 70 Å channel, which functions to sequester CO and facilitate its movement to the ACS active site.[184] This channel has been identified biochemically[185,186] and by X-ray crystallography.[170,172]

Like CODH, the catalytic strategy of ACS is to use a Ni active site to form organometallic intermediates. The active site of ACS, the A-cluster, was the first published example of a NiFeS cluster.[187] It consists of a [4Fe−4S] cluster bridged to a Ni site (Ni_p) that is thiolate-bridged to another Ni ion in a thiolato- and carboxamido-type N_2S_2 coordination environment (Figure 28).[170,172,188] Thus, one can describe the A-cluster as a binuclear NiNi center bridged by a cysteine residue (Cys509) to a [4Fe−4S] cluster. This arrangement is similar to the Fe-only hydrogenases in which a [4Fe−4S] cluster and a binuclear Fe site are bridged by a Cys residue.[189,190]

A proposed mechanism for ACS is described in Figure 29. Several reviews that focus on the structure, function, and mechanism of ACS are available.[191−194] An alternative mechanism involving a Ni(0) state and all diamagnetic intermediates has been proposed and is described fully in a recent review.[191] The difference between the two mechanisms is primarily in the assignment of the electronic structure of

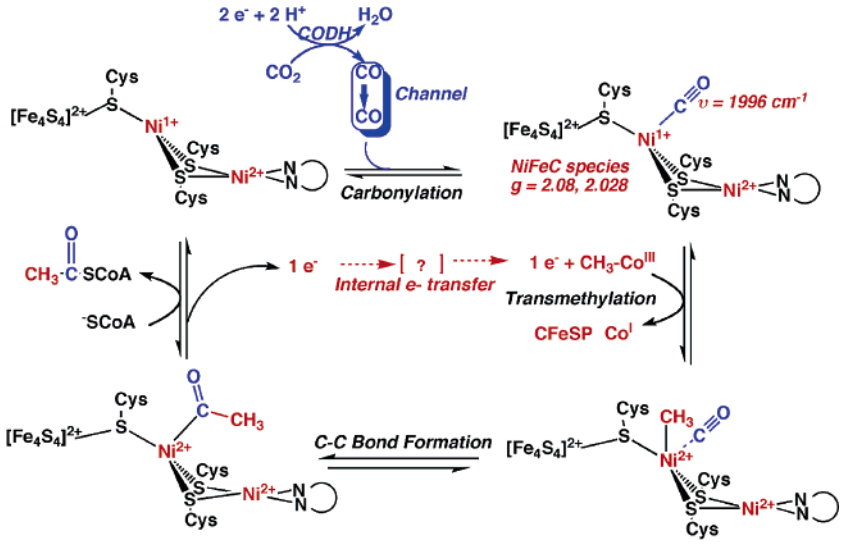

Figure 29. Proposed mechanism for ACS.

the intermediates, so for the current review, I will describe the series of steps in only what has become called the "paramagnetic mechanism", so-called because the proposed key intermediate (the NiFeC species) is paramagnetic and EPR active. Another point of discussion is whether CO or the methyl group is first to bind to the Ni center. In this review, I will describe only the following binding sequence: CO, then methyl, then CoA.

Preceding the first step are two "priming" reactions. The first is CO migration through the channel from cluster C to concentrate near cluster A, and the second priming step is the reductive activation of ACS. Then, in the first step in the ACS mechanism, the Carbonylation Step, cluster A reacts with CO to form an organometallic complex, called the NiFeC species (Figure 29). The NiFeC species is characterized by an EPR signal that forms (when treated with CO) and decays (upon reaction with the methyl group donor) at a rate consistent with its involvement as a catalytic intermediate in acetyl-CoA synthesis.[195,196] On the basis of computational studies, the electronic structure of the A-cluster in this paramagnetic state is best described as a $[4Fe-4S]^{2+}$ cluster linked to a Ni^{1+} center at the proximal metal (M_p) site. In turn, Ni_p is bridged to another Ni^{2+} (Ni_d) that is distal to the FeS cluster.[197] The unpaired spin density in this complex resides predominantly on Ni_p, with some delocalization into the terminal carbonyl group, based on the observation of ^{13}CO hyperfine splittings in the EPR signal.[187,198] Thus, one role of the low-valent Ni center in ACS—to bind CO—is reminiscent of CO binding to a low-valent ferrous site in heme proteins.

The next step in the ACS mechanism is methylation of the A-cluster. This reaction involves the corrinoid iron–sulfur protein (CFeSP), which will be described in the next section on cobalamin-dependent methyltransferases. The recent crystal structures reveal ACS in open and closed states, and in the closed state, the A-cluster is inaccessible for binding another protein, implying that a major conformational change occurs during the catalytic cycle. There is evidence that the methyl group binds to the labile Ni site of the A-cluster[199,200] that, based on XAS studies, appears to be Ni_p.[201]

The transmethylation reaction could occur by transfer of a methyl radical or an S_N2-type nucleophilic mechanism involving a methyl cation. Model studies of the reaction between methyl-Co^{3+} (CH_3-Co^{3+} dimethylglyoximate) and a Ni^{1+} macrocycle indicate that transfer of a methyl radical is favored.[202,203] A radical methyl transfer would require homolysis of the CH_3-Co bond of the methylated CFeSP, which Finke et al. suggested could not occur because reduction of CH_3-Co^{3+} requires redox potentials (<-1 V) that are too low for physiological electron donors.[204] Rapid kinetic studies and stereochemical studies using a chiral methyl donor also indicate that the transmethylation reaction involves an S_N2-type nucleophilic attack of Ni_p on the methyl group of the methylated CFeSP (CH_3-Co^{3+}) to generate methyl-Ni and Co^{1+}.[205−207] However, methyl-Ni is diamagnetic, suggesting a methyl-Ni^{2+} state,[195,200] and indicating that the S_N2 "methyl cation" transfer precedes (or is linked to) a one-electron transfer (Figure 29) (since methyl-Ni^{3+} would be EPR active). Thus, linking the S_N2 reaction to an electron-transfer step would be equivalent to a radical methyl transfer. Since it is clear that the ACS reaction does not require net input of electrons,[208] Figure 29 proposes that the electron that is donated during the methylation step is returned at a latter step in the reaction (after CoA binds).

The next step in the ACS mechanism involves carbon–carbon bond formation, which occurs by condensation of the methyl and carbonyl groups to form an acetyl-metal species. Then, the final steps in the catalytic cycle involve binding of CoA and thiolysis of the acetyl-metal bond. There is evidence that the sulfur of CoA binds to the proximal metal site in the A-cluster, by EXAFS studies of the binding of seleno-CoA to CODH/ACS.[209]

In summary, the ACS catalytic cycle appears to involve metal-centered catalysis involving bioorganometallic intermediates that resemble the Monsanto process for industrial acetate production. Both reactions appear to occur through methyl-metal, metal-CO, and acetyl-metal intermediates. The use of a low-valent metal center as a nucleophile is rare in biochemistry and is reminiscent of the reactions of cobalamin-dependent methyltransferases such as methionine synthase.[29,210] In fact, kinetic studies indicate that the Ni^{1+} site on ACS appears to be about as effective as Co^{1+}-CFeSP as a methyl group acceptor.[211]

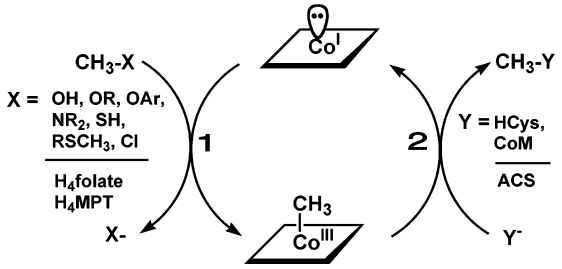

Figure 30. Cobalamin-dependent methyltransferases.

2.3.3. Cobalt as a Supernucleophile in Cobalamin-Dependent Methyltransferases

The preceding section described the methylation of ACS by the methylated CFeSP, which involves the use of low-valent nickel as a nucleophile. There is another well-characterized biological system that uses the cobalt ion at the center of vitamin B_{12} (cobalamin) as a nucleophile: the cobalamin-dependent methyltransferase. Adenosylcobalamin was introduced earlier (Figure 4); however, this form of cobalamin appears to be used only in radical reactions. Cobalamin also is found in Nature in the cyano-, hydroxy-, and methylcobalamin forms in Vitamin B_{12}, hydroxycobalamin, and methylcobalamin; however, the natural occurrence of cyanocobalamin is debated. The methyltransferases use a low-valent Co^{1+} state (in which both the upper and lower axial positions are vacant) as the nucleophile and generate methylcobalamin (methyl-Co^{3+}). This class of methyltransferases has been recently reviewed.[29]

Cobalamin-dependent methyltransferases catalyze the transfer of a methyl group from a methyl donor to a methyl group acceptor (Figure 30), where X and Y are the leaving group and the nucleophile, respectively. Cobalamin cycles between the Co^{1+} and methyl-Co^{3+} states, undergoing a cycle of methylation by the methyl donor followed by demethylation as it transfers its methyl group to a methyl group acceptor. Among the various methyltransferases, CH_3X can designate methanol, methylated amines, methylated thiols, methoxylated aromatics, methylated heavy metals, methyltetrahydrofolate (CH_3-H_4folate), or the methanogenic analogue, methyltetrahydromethanopterin (CH_3-H_4MPT). The known methyl acceptors (Y) consist of homocysteine, Coenzyme M, or as described in the previous section, the Ni^{1+} site on the A-cluster of ACS.

Methionine synthase (MetH) is the most extensively studied cobalamin-dependent methyltransferase. This enzyme catalyzes the transfer of the methyl group from CH_3-H_4folate to homocysteine to form methionine and H_4folate with an enzyme enhancement factor of 35 million.[210,212] In many of the methyltransferases, the domains for binding X, Y, and cobalamin (Figure 30) are found on different proteins; however, all of these domains, plus a separate activation domain that binds *S*-adenosylmethionine, are located in a modular fashion on methionine synthase. Since the cobalamin domain is the central player in the methyl transfer reactions, this Co center in its different oxidation states must undergo a series of molecular juggling acts during each catalytic cycle to accomplish the following interactions: the Co(I) form with the CH_3-H_4folate binding domain, the Co(II) form with the AdoMet binding domain, and the CH_3-Co(III) form with the homocysteine binding domain. Given the complexity of these large-scale movements, it is perhaps not surprising that the various conformational changes required during catalysis are rate-limiting during steady-state turnover.[210]

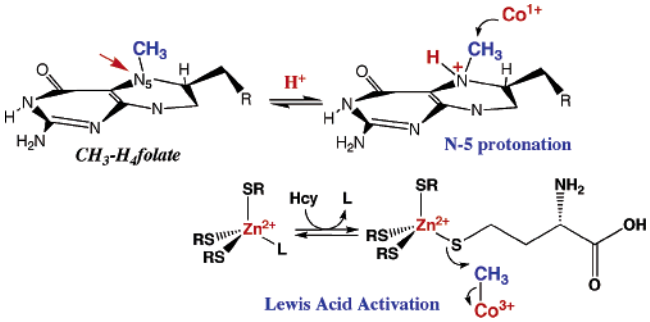

Figure 31. Activation of the substrate in cobalamin-dependent methyltransferases. HCy = homocysteine.

The independent "modules" of methionine synthase retain most of their functional activity and have been individually expressed and characterized.[213] Crystallization of the cobalamin binding domain led to the first structure of a protein-bound cobalamin, in which the lower axial benzimidazole ligand shown in Figure 4 is replaced by a histidine residue from the protein.[214] This arrangement is called the "His-on" conformation and is found in many methyltransferases (as well as in many adenosylcobalamin-dependent enzymes). Furthermore, the histidine ligand is part of a triad of residues (H759, D757, and S810) that control the coordination state of cobalt, that is, "His-on" or "His-off", by modulating the protonation state of the histidine. The N-terminal CH_3-H_4-folate and homocysteine[215] and the C-terminal SAM binding domains[216] also have been crystallized.

The CH_3-H_4folate binding domain of methionine synthase is homologous to the cobalamin-dependent methyltransferase (MeTr) that methylates the CFeSP, which donates the methyl group to ACS (described in the previous section on ACS). In this system, the MeTr is an independent protein that, like the CH_3-H_4folate binding domain of methionine synthase and other methyl donor binding domains, assumes an $(\alpha\beta)_8$ TIM barrel fold.[217] The CFeSP contains an iron−sulfur cluster that functions in reductive activation of the cobalt center from the Co^{2+} to the Co^{1+} state.[205,206] This is important because, about once in every 100 turnovers, the cobalt center undergoes oxidation to the inactive Co^{2+} state.

The methyl groups in the various methyl donors shown in Figure 29 are not sufficiently electrophilic to undergo nucleophilic attack, even by a potent supernucleophile (Co^{1+}). In the case of CH_3-H_4folate, it appears that electrophilic activation of the leaving group (H_4folate) occurs by protonation of the N5 group to which the methyl group is bound (Figure 31).[218−220]

For the methyl thiolates and methanol (Figure 31), electrophilic activation appears to occur by coordination of the heteroatom of the methyl donor substrate to a Lewis acid. This activation mechanism, which has been best studied in methionine synthase, involves coordination of the thiol group of homocysteine to Zn in a $(Cys)_3Zn^{2+}$ cluster within the N-terminal homocysteine binding domain.[221] The Zn complex acts as a Lewis acid to deprotonate the thiol group, and as a thiolate reservoir from which homocysteinate can dissociate and react with methyl-Co^{3+} in a nucleophilic addition reaction to generate methionine. The activation of thiols to catalyze nucleophilic additions has also been proposed in other proteins including the Ada methyltransferase[222] and farnesyltransferase.[223] All of the methyltransferases that catalyze methylation of thiol substrates appear to contain Zn, suggesting a similar mode of substrate activation.

3. Conclusions and Outlook

Metal ions catalyze a diverse array of reactions, many of which take advantage of the ability of transition metals to switch among various redox and coordination states. This review has covered some of the major strategies used by metalloenzymes to accomplish difficult transformations. The mononuclear iron, diiron, and heme-containing oxygenases catalyze the generation of high-valent metal-oxo intermediates that perform hydrogen atom abstraction and oxygenation reactions. On the other hand, enzymes that contain adenosylcobalamin and adenosylmethionine promote Co−C and C−S bond homolysis, leading to the formation of a catalytic adenosyl radical that promotes H-atom abstraction from a substrate or amino acid residue. The role of the metal is different in these two classes of reactions. In the adenosylcobalamin-dependent enzymes, the metal center serves as a reservoir for the latent adenosyl radical, while a [4Fe−4S] cluster donates an electron to initiate C−S bond cleavage in the radical SAM enzymes. In several enzymes, low-valent metal ions act as nucleophiles, forming organometallic intermediates and undergoing transformations that are reminiscent of some well-studied and industrially important inorganic reactions such as the Monsanto Process and the Water−Gas Shift Reaction. In many of the reactions described in this review, the primary scaffold (the first coordination sphere) undergoes mechanistically significant movements. Furthermore, the extended scaffold (the protein) often undergoes large conformational changes, which move the metal center over large distances during the reaction cycle. This coordinated molecular acrobatics can place the metal center in contact with a redox activation module at one reaction step and in juxtaposition with domains responsible for binding different substrates at other stages of the catalytic cycle.

Another component of the extended scaffold is to provide a molecular "wire" near the catalytic center. In the specific examples of CODH and PFOR, the electron-transfer chain has a major impact on the nature of the reaction. In both cases, the wires consist of FeS clusters each separated by 9−12 Å, which is a suitable distance for extremely rapid ($>1000\ s^{-1}$) electron-transfer reaction.[180,224] In the absence of a redox wire near the HE-TPP intermediate, PFOR would likely become a pyruvate decarboxylase, generating acetaldehyde instead of acetyl-CoA and two electrons. This would be detrimental to the cell, since the two reducing equivalents that are produced allow the PFOR reaction to drive the reduction of ferredoxin and other low-potential electron carriers involved in microbial energy generation. Similarly, in the absence of the wire, the CODH mechanism would probably more closely resemble that of the water−gas shift reaction, converting CO to CO_2 to produce H_2, instead of reduced ferredoxin.

4. Acknowledgments

The author thanks DOE (DE-FG03-ER20297) and NIH (GM39451) for partial support of this work. The author thanks John Lipscomb, Paul Ortiz de Montellano, Perry Frey, and Steve Lippard for their extremely helpful comments, suggestions, and critiques of an early draft of this paper. The author also thanks Amy Rosenzweig, Matt Sazinsky, and Wolfgang Buckel for helpful discussions related to the manuscript. He is grateful to those past and present members of his laboratory for their contribution to metalloenzyme research.

5. References

(1) Sumner, J. B. *J. Biol. Chem.* **1926**, *69*, 435.
(2) Dixon, N. E.; Gazzola, C.; Blakeley, R. L.; Zerner, B. *J. Am. Chem. Soc.* **1975**, *97*, 4131.
(3) Kovacs, J. A. *Chem. Rev.* **2004**, *104*, 825.
(4) Jensen, K. P.; Ryde, U. *J. Porphyrins Phthalocyanines* **2005**, *9*, 581.
(5) Kolberg, M.; Strand, K. R.; Graff, P.; Andersson, K. K. *Biochim. Biophys. Acta* **2004**, *1699*, 1.
(6) Strand, K. R.; Karlsen, S.; Kolberg, M.; Rohr, A. K.; Gorbitz, C. H.; Andersson, K. K. *J. Biol. Chem.* **2004**, *279*, 46794.
(7) Whittington, D. A.; Lippard, S. J. *J. Am. Chem. Soc.* **2001**, *123*, 827.
(8) Frazee, R. W.; Orville, A. M.; Dolbeare, K. B.; Yu, H.; Ohlendorf, D. H.; Lipscomb, J. D. *Biochemistry* **1998**, *37*, 2131.
(9) Roach, P. L.; Clifton, I. J.; Hensgens, C. M.; Shibata, N.; Schofield, C. J.; Hajdu, J.; Baldwin, J. E. *Nature* **1997**, *387*, 827.
(10) Schindelin, H.; Kisker, C.; Hilton, J.; Rajagopalan, K. V.; Rees, D. C. *Science* **1996**, *272*, 1615.
(11) Williams, P. A.; Fulop, V.; Garman, E. F.; Saunders: N. F.; Ferguson, S. J.; Hajdu, J. *Nature* **1997**, *389*, 406.
(12) Xie, J.; Yikilmaz, E.; Miller, A. F.; Brunold, T. C. *J. Am. Chem. Soc.* **2002**, *124*, 3769.
(13) Jackson, T. A.; Brunold, T. C. *Acc. Chem. Res.* **2004**, *37*, 461.
(14) Wirstam, M.; Lippard, S. J.; Friesner, R. A. *J. Am. Chem. Soc.* **2003**, *125*, 3980.
(15) Phillips, S. E.; Schoenborn, B. P. *Nature* **1981**, *292*, 81.
(16) Schenk, G.; Neidig, M. L.; Zhou, J.; Holman, T. R.; Solomon, E. I. *Biochemistry* **2003**, *42*, 7294.
(17) McCall, K. A.; Huang, C.; Fierke, C. A. *J. Nutr.* **2000**, *130*, 1437S.
(18) Kiefer, L. L.; Krebs, J. F.; Paterno, S. A.; Fierke, C. A. *Biochemistry* **1993**, *32*, 9896.
(19) Lesburg, C. A.; Huang, C.; Christianson, D. W.; Fierke, C. A. *Biochemistry* **1997**, *36*, 15780.
(20) Liang, Z.; Xue, Y.; Behravan, G.; Jonsson, B. H.; Lindskog, S. *Eur. J. Biochem.* **1993**, *211*, 821.
(21) Hunt, J. A.; Ahmed, M.; Fierke, C. A. *Biochemistry* **1999**, *38*, 9054.
(22) Levine, H. L.; Brody, R. S.; Westheimer, F. H. *Biochemistry* **1980**, *19*, 4993.
(23) Miller, B. G.; Hassell, A. M.; Wolfenden, R.; Milburn, M. V.; Short, S. A. *Proc. Natl. Acad. Sci. U.S.A.* **2000**, *97*, 2011.
(24) Stubbe, J.; Nocera, D. G.; Yee, C. S.; Chang, M. C. *Chem. Rev.* **2003**, *103*, 2167.
(25) Ragsdale, S. W. *Chem. Rev.* **2003**, *103*, 2333.
(26) Frey, P. A.; Magnusson, O. T. *Chem. Rev.* **2003**, *103*, 2129.
(27) Toraya, T. *Chem. Rev.* **2003**, *103*, 2095.
(28) Toraya, T. *Cell. Mol. Life Sci.* **2000**, *57*, 106.
(29) Banerjee, R.; Ragsdale, S. W. *Annu. Rev. Biochem.* **2003**, *72*, 209.
(30) Reed, G. H. *Curr. Opin. Chem. Biol.* **2004**, *8*, 477.
(31) *Radical Enzymology*; Banerjee, R., Ed.; American Chemical Society: Washington, DC, 2003; Vol. 103.
(32) Reichard, P.; Ehrenberg, A. *Science* **1983**, *221*, 514.
(33) Hay, B. P.; Finke, R. G. *J. Am. Chem. Soc.* **1987**, *109*, 8012.
(34) Brown, K. L.; Zou, X. *J. Inorg. Biochem.* **1999**, *77*, 185.
(35) Padmakumar, R.; Padmakumar, R.; Banerjee, R. *Biochemistry* **1997**, *36*, 3713.
(36) Bandarian, V.; Reed, G. H. *Biochemistry* **2000**, *39*, 12069.
(37) Licht, S. S.; Booker, S.; Stubbe, J. *Biochemistry* **1999**, *38*, 1221.
(38) Marsh, E. N. G.; Ballou, D. P. *Biochemistry* **1998**, *37*, 11864.
(39) Cheng, M. C.; Marsh, E. N. *Biochemistry* **2005**, *44*, 2686.
(40) Gruber, K.; Kratky, C. *Curr. Opin. Chem. Biol.* **2002**, *6*, 598.
(41) Banerjee, R. *Chem. Rev.* **2003**, *103*, 2083.
(42) Lawrence, C. C.; Stubbe, J. *Curr. Opin. Chem. Biol.* **1998**, *2*, 650.
(43) Sintchak, M. D.; Arjara, G.; Kellogg, B. A.; Stubbe, J.; Drennan, C. L. *Nat. Struct. Biol.* **2002**, *9*, 293.
(44) Layer, G.; Heinz, D. W.; Jahn, D.; Schubert, W. D. *Curr. Opin. Chem. Biol.* **2004**, *8*, 468.
(45) Frey, P. A.; Booker, S. J. *Adv. Protein Chem.* **2001**, *58*, 1.
(46) Cheek, J.; Broderick, J. B. *J. Biol. Inorg. Chem.* **2001**, *6*, 209.
(47) Walsby, C. J.; Ortillo, D.; Yang, J.; Nnyepi, M. R.; Broderick, W. E.; Hoffman, B. M.; Broderick, J. B. *Inorg. Chem.* **2005**, *44*, 727.
(48) Lepore, B. W.; Ruzicka, F. J.; Frey, P. A.; Ringe, D. *Proc. Natl. Acad. Sci. U.S.A.* **2005**, *102*, 13819.
(49) Nicolet, Y.; Drennan, C. L. *Nucleic Acids Res.* **2004**, *32*, 4015.
(50) Walsby, C. J.; Hong, W.; Broderick, W. E.; Cheek, J.; Ortillo, D.; Broderick, J. B.; Hoffman, B. M. *J. Am. Chem. Soc.* **2002**, *124*, 3143.
(51) Buis, J. M.; Broderick, J. B. *Arch. Biochem. Biophys.* **2005**, *433*, 288.
(52) Knappe, J.; Blaschkowski, H. P. *Methods Enzymol.* **1975**, *41B*, 508.

(53) Frey, M.; Rothe, M.; Wagner, A. F.; Knappe, J. *J. Biol. Chem.* **1994**, *269*, 12432.
(54) Washabaugh, M. W.; Jencks, W. P. *Biochemistry* **1988**, *27*, 5044.
(55) Breslow, R. *J. Am. Chem. Soc.* **1957**, *80*, 3719.
(56) Breslow, R. *J. Am. Chem. Soc.* **1957**, *79*, 1762.
(57) Schellenberger, A. *Biochim. Biophys. Acta* **1998**, *1385*, 177.
(58) Furdui, C.; Ragsdale, S. W. *Biochemistry* **2002**, *41*, 9921.
(59) Chabriere, E.; Charon, M.-H.; Volbeda, A.; Pieulle, L.; Hatchikian, E. C.; Fontecilla-Camps, J.-C. *Nat. Struct. Biol.* **1999**, *6*, 182.
(60) Tittmann, K.; Wille, G.; Golbik, R.; Weidner, A.; Ghisla, S.; Hubner, G. *Biochemistry* **2005**, *44*, 13291.
(61) Astashkin, A. V.; Seravalli, J.; Mansoorabadi, S. O.; Reed, G. H.; Ragsdale, S. W. *J. Am. Chem. Soc.* **2006**, *128*, 3888.
(62) Chabriere, E.; Vernede, X.; Guigliarelli, B.; Charon, M. H.; Hatchikian, E. C.; Fontecilla-Camps, J. C. *Science* **2001**, *294*, 2559.
(63) Mansoorabadi, S. O.; Seravalli, J.; Furdui, C.; Krymov, V.; Gerfen, G. J.; Begley, T. P.; Melnick, J.; Ragsdale, S. W.; Reed, G. H. *Biochemistry* **2006**, *45*, 7122.
(64) Frey, P. A. *Science* **2001**, *294*, 2489.
(65) Buckel, W. *Appl. Microbiol. Biotechnol.* **2001**, *57*, 263.
(66) Hans, M.; Bill, E.; Cirpus, I.; Pierik, A. J.; Hetzel, M.; Alber, D.; Buckel, W. *Biochemistry* **2002**, *41*, 5873.
(67) Smith, D. M.; Buckel, W.; Zipse, H. *Angew. Chem., Int. Ed.* **2003**, *42*, 1867.
(68) Buckel, W.; Martins, B. M.; Messerschmidt, A.; Golding, B. T. *Biol. Chem.* **2005**, *386*, 951.
(69) Kovacs, J. A. *Science* **2003**, *299*, 1024.
(70) Koehntop, K. D.; Emerson, J. P.; Que, L., Jr. *J. Biol. Inorg. Chem.* **2005**, *10*, 87.
(71) Hausinger, R. P. *Crit. Rev. Biochem. Mol. Biol.* **2004**, *39*, 21.
(72) Bassan, A.; Blomberg, M. R.; Siegbahn, P. E. *J. Biol. Inorg. Chem.* **2004**, *9*, 439.
(73) Ryle, M. J.; Padmakumar, R.; Hausinger, R. P. *Biochemistry* **1999**, *38*, 15278.
(74) Price, J. C.; Barr, E. W.; Tirupati, B.; Bollinger, J. M., Jr.; Krebs, C. *Biochemistry* **2003**, *42*, 7497.
(75) Price, J. C.; Barr, E. W.; Glass, T. E.; Krebs, C.; Bollinger, J. M., Jr. *J. Am. Chem. Soc.* **2003**, *125*, 13008.
(76) Price, J. C.; Barr, E. W.; Hoffart, L. M.; Krebs, C.; Bollinger, J. M., Jr. *Biochemistry* **2005**, *44*, 8138.
(77) Wallar, B. J.; Lipscomb, J. D. *Chem. Rev.* **1996**, *96*, 2625.
(78) Rosenzweig, A. C.; Frederick, C. A.; Lippard, S. J.; Nordlund, P. *Nature* **1993**, *366*, 537.
(79) Lieberman, R. L.; Rosenzweig, A. C. *Crit. Rev. Biochem. Mol. Biol.* **2004**, *39*, 147.
(80) Lieberman, R. L.; Rosenzweig, A. C. *Nature* **2005**, *434*, 177.
(81) Liu, Y.; Nesheim, J. C.; Lee, S. K.; Lipscomb, J. D. *J. Biol. Chem.* **1995**, *270*, 24662.
(82) Lee, S. K.; Lipscomb, J. D. *Biochemistry* **1999**, *38*, 4423.
(83) Lee, S. K.; Nesheim, J. C.; Lipscomb, J. D. *J. Biol. Chem.* **1993**, *268*, 21569.
(84) Baik, M. H.; Newcomb, M.; Friesner, R. A.; Lippard, S. J. *Chem. Rev.* **2003**, *103*, 2385.
(85) Merkx, M.; Kopp, D. A.; Sazinsky, M. H.; Blazyk, J. L.; Müller, J.; Lippard, S. J. *Angew. Chem., Int. Ed.* **2001**, *40*, 2782.
(86) Walters, K. J.; Gassner, G. T.; Lippard, S. J.; Wagner, G. *Proc. Natl. Acad. Sci. U.S.A.* **1999**, *96*, 7877.
(87) Chang, S. L.; Wallar, B. J.; Lipscomb, J. D.; Mayo, K. H. *Biochemistry* **1999**, *38*, 5799.
(88) Chatwood, L. L.; Muller, J.; Gross, J. D.; Wagner, G.; Lippard, S. J. *Biochemistry* **2004**, *43*, 11983.
(89) Muller, J.; Lugovskoy, A. A.; Wagner, G.; Lippard, S. J. *Biochemistry* **2002**, *41*, 42.
(90) Zhang, J.; Lipscomb, J. D. *Biochemistry* **2006**, *45*, 1459.
(91) Rosenzweig, A. C.; Brandstetter, H.; Whittington, D. A.; Nordlund, P.; Lippard, S. J.; Frederick, C. A. *Proteins* **1997**, *29*, 141.
(92) Sazinsky, M. H.; Lippard, S. J. *J. Am. Chem. Soc.* **2005**, *127*, 5814.
(93) Shu, L.; Nesheim, J. C.; Kauffmann, K.; Munck, E.; Lipscomb, J. D.; Que, L., Jr. *Science* **1997**, *275*, 515.
(94) Fox, B. G.; Borneman, J. G.; Wackett, L. P.; Lipscomb, J. D. *Biochemistry* **1990**, *29*, 6419.
(95) Groves, J. T.; McClusky, G. A. *J. Am. Chem. Soc.* **1976**, *98*, 859.
(96) Nesheim, J. C.; Lipscomb, J. D. *Biochemistry* **1996**, *35*, 10240.
(97) Lipscomb, J. D.; Que, J. L. *J. Biol. Inorg. Chem.* **1998**, *3*, 331.
(98) Priestley, N.; Floss, H. G.; Froland, W.; Lipscomb, J. D.; Williams, P. G.; Morimoto, H. *J. Am. Chem. Soc.* **1992**, *114*, 4.
(99) Gherman, B. F.; Lippard, S. J.; Friesner, R. A. *J. Am. Chem. Soc.* **2005**, *127*, 1025.
(100) Brazeau, B. J.; Lipscomb, J. D. *Biochemistry* **2000**, *39*, 13503.
(101) Deighton, N.; Podmore, I. D.; Symons, M. C. R.; Wilkins, P. C.; Dalton, H. *J. Chem. Soc. Chem. Commun.* **1991**, 1086.
(102) Liu, A.; Jin, Y.; Zhang, J.; Brazeau, B. J.; Lipscomb, J. D. *Biochem. Biophys. Res. Commun.* **2005**, *338*, 254.
(103) Jin, Y.; Lipscomb, J. D. *Biochim. Biophys. Acta* **2000**, *1543*, 47.
(104) Maines, M. D. *Antioxid. Redox Signaling* **2004**, *6*, 797.
(105) Maines, M. D. *Physiology* **2005**, *20*, 382.
(106) Colas, C.; Ortiz de Montellano, P. R. *Chem. Rev.* **2003**, *103*, 2305.
(107) Wilks, A. *Antioxid. Redox Signaling* **2002**, *4*, 603.
(108) Montellano, P. R. *Curr. Opin. Chem. Biol.* **2000**, *4*, 221.
(109) Auclair, K.; Ortiz de Montellano, P. R. In *Porphyrin Handbook*; Kadish, K., Smith, K., Guilard, R., Ed.; Academic Press: New York, 2003; Vol. 12.
(110) Rhie, G.; Beale, S. I. *Arch. Biochem. Biophys.* **1995**, *320*, 182.
(111) Willows, R. D.; Mayer, S. M.; Foulk, M. S.; DeLong, A.; Hanson, K.; Chory, J.; Beale, S. I. *Plant Mol. Biol.* **2000**, *43*, 113.
(112) Ratliff, M.; Zhu, W.; Deshmukh, R.; Wilks, A.; Stojiljkovic, I. *J. Bacteriol.* **2001**, *183*, 6394.
(113) Ortiz de Montellano, P. *Acc. Chem. Res.* **1998**, *31*, 543.
(114) Qi, Z.; Hamza, I.; O'Brian, M. R. *Proc. Natl. Acad. Sci. U.S.A.* **1999**, *96*, 13056.
(115) Ogawa, K.; Sun, J.; Taketani, S.; Nakajima, O.; Nishitani, C.; Sassa, S.; Hayashi, N.; Yamamoto, M.; Shibahara, S.; Fujita, H.; Igarashi, K. *EMBO J.* **2001**, *20*, 2835.
(116) Dioum, E. M.; Rutter, J.; Tuckerman, J. R.; Gonzalez, G.; Gilles-Gonzalez, M. A.; McKnight, S. L. *Science* **2002**, *298*, 2385.
(117) Hantke, K. *Curr. Opin. Microbiol.* **2001**, *4*, 172.
(118) Eisenstein, R. S.; Blemings, K. P. *J. Nutr.* **1998**, *128*, 2295.
(119) Stocker, R.; Yamamoto, Y.; McDonagh, A. F.; Glazer, A. N.; Ames, B. N. *Science* **1987**, *235*, 1043.
(120) Baranano, D. E.; Snyder, S. H. *Proc. Natl. Acad. Sci. U.S.A.* **2001**, *98*, 10996.
(121) Williams, S. E.; Wootton, P.; Mason, H. S.; Bould, J.; Iles, D. E.; Riccardi, D.; Peers, C.; Kemp, P. J. *Science* **2004**, *306*, 2093.
(122) Wilks, A.; Torpey, J.; Ortiz de Montellano, P. R. *J. Biol. Chem.* **1994**, *269*, 29553.
(123) Takahashi, S.; Ishikawa, K.; Takeuchi, N.; Ikeda-Saito, M.; Yoshida, T.; Rousseau, D. L. *J. Am. Chem. Soc.* **1995**, *117*, 6002.
(124) Wilks, A.; Ortiz de Montellano, P. R. *J. Biol. Chem.* **1993**, *268*, 22357.
(125) Uzawa, T.; Kimura, T.; Ishimori, K.; Morishima, I.; Matsui, T.; Ikeda-Saito, M.; Takahashi, S.; Akiyama, S.; Fujisawa, T. *J. Mol. Biol.* **2006**, *357*, 997.
(126) Fujii, H.; Zhang, X.; Tomita, T.; Ikeda-Saito, M.; Yoshida, T. *J. Am. Chem. Soc.* **2001**, *123*, 6475.
(127) Li, Y.; Syvitski, R. T.; Auclair, K.; Wilks, A.; Ortiz de Montellano, P. R.; La Mar, G. N. *J. Biol. Chem.* **2002**, *277*, 33018.
(128) Matsui, T.; Furukawa, M.; Unno, M.; Tomita, T.; Ikeda-Saito, M. *J. Biol. Chem.* **2005**, *280*, 2981.
(129) Liu, Y.; Koenigs Lightning, L.; Huang, H.; Moenne-Loccoz, P.; Schuller, D. J.; Poulos, T. L.; Loehr, T. M.; Ortiz de Montellano, P. R. *J. Biol. Chem.* **2000**, *275*, 34501.
(130) Sugishima, M.; Sakamoto, H.; Higashimoto, Y.; Omata, Y.; Hayashi, S.; Noguchi, M.; Fukuyama, K. *J. Biol. Chem.* **2002**, *277*, 45086.
(131) Matsui, T.; Nakajima, A.; Fujii, H.; Matera, K. M.; Migita, C. T.; Yoshida, T.; Ikeda-Saito, M. *J. Biol. Chem.* **2005**, *280*, 36833.
(132) Liu, Y.; Ortiz de Montellano, P. R. *J. Biol. Chem.* **2000**, *275*, 5297.
(133) Unno, M.; Matsui, T.; Chu, G. C.; Couture, M.; Yoshida, T.; Rousseau, D. L.; Olson, J. S.; Ikeda-Saito, M. *J. Biol. Chem.* **2004**, *279*, 21055.
(134) DiMarco, A. A.; Bobik, T. A.; Wolfe, R. S. *Annu. Rev. Biochem.* **1990**, *59*, 355.
(135) Ellermann, J.; Kobelt, A.; Pfaltz, A.; Thauer, R. K. *FEBS Lett.* **1987**, *220*, 358.
(136) Thauer, R. K. *Microbiology* **1998**, *144*, 2377.
(137) Diekert, G.; Klee, B.; Thauer, R. K. *Arch. Microbiol.* **1980**, *124*, 103.
(138) Diekert, G.; Jaenchen, R.; Thauer, R. K. *FEBS Lett.* **1980**, *119*, 118.
(139) Whitman, W. B.; Wolfe, R. S. *Biochem. Biophys. Res. Commun.* **1980**, *92*, 1196.
(140) Ermler, U.; Grabarse, W.; Shima, S.; Goubeaud, M.; Thauer, R. K. *Science* **1997**, *278*, 1457.
(141) Pfaltz, A.; Juan, B.; Fassler, A.; Eschenmoser, A.; Jaenchen, R.; Gilles, H. H.; Diekert, G.; Thauer, R. K. *Helv. Chim. Acta* **1982**, *65*, 828.
(142) Färber, G.; Keller, W.; Kratky, C.; Jaun, B.; Pfaltz, A.; Spinner, C.; Kobelt, A.; Eschenmoser, A. *Helv. Chim. Acta* **1991**, *74*, 697.
(143) Holliger, C.; Pierik, A. J.; Reijerse, E. J.; Hagen, W. R. *J. Am. Chem. Soc.* **1993**, *115*, 5651.
(144) Telser, J. In *Structure and Bonding*; Williams, R. J. P., Ed.; Springer-Verlag: Heidelberg, Germany, 1998; Vol. 91.
(145) Grabarse, W. G.; Mahlert, F.; Duin, E. C.; Goubeaud, M.; Shima, S.; Thauer, R. K.; Lamzin, V.; Ermler, U. *J. Mol. Biol.* **2001**, *309*, 315.
(146) Maki, A. H.; Edelstein, N.; Davison, A.; Holm, R. H. *J. Am. Chem. Soc.* **1964**, *86*, 4580.

(147) Telser, J.; Horng, Y. C.; Ragsdale, S. W.; Hoffman, B. M. Unpublished work, 2006.

(148) Ragsdale, S. W. In *The Porphyrin Handbook*; Kadish, K. M., Smith, K. M., Guilard, R., Eds.; Academic Press: New York, 2003; Vol. 11.
(149) Craft, J. L.; Horng, Y.-C.; Ragsdale, S. W.; Brunold, T. C. *J. Am. Chem. Soc.* **2004**, *126*, 4068.
(150) Craft, J. L.; Horng, Y. C.; Ragsdale, S. W.; Brunold, T. C. *J. Biol. Inorg. Chem.* **2004**, *9*, 77.
(151) Harmer, J.; Finazzo, C.; Piskorski, R.; Bauer, C.; Jaun, B.; Duin, E. C.; Goenrich, M.; Thauer, R. K.; Van Doorslaer, S.; Schweiger, A. *J. Am. Chem. Soc.* **2005**, *127*, 17744.
(152) Horng, Y.-C.; Becker, D. F.; Ragsdale, S. W. *Biochemistry* **2001**, *40*, 12875.
(153) Goubeaud, M.; Schreiner, G.; Thauer, R. K. *Eur. J. Biochem.* **1997**, *243*, 110.
(154) Siegbahn, P. E. *Q. Rev. Biophys.* **2003**, *36*, 91.
(155) Lin, S.-K.; Jaun, B. *Helv. Chim. Acta* **1991**, *74*, 1725.
(156) Lin, S.-K.; Jaun, B. *Helv. Chim. Acta* **1992**, *75*.
(157) Jaun, B.; Pfaltz, A. *J. Chem. Soc. Chem. Commun.* **1988**, *1327*, 293.
(158) Signor, L.; Knuppe, C.; Hug, R.; Schweizer, B.; Pfaltz, A.; Jaun, B. *Chemistry* **2000**, *6*, 3508.
(159) Pelmenschikov, V.; Blomberg, M. R. A.; Siegbahn, P. E. M.; Crabtree, R. H. *J. Am. Chem. Soc.* **2002**, *124*, 4039.
(160) Bartholomew, G. W.; Alexander, M. *Appl. Environ. Microbiol.* **1979**, *37*, 932.
(161) Ragsdale, S. W. *CRC Crit. Rev. Biochem. Mol. Biol.* **2004**, *39*, 165.
(162) Svetlitchnyi, V.; Peschel, C.; Acker, G.; Meyer, O. *J. Bacteriol.* **2001**, *183*, 5134.
(163) Grahame, D. A.; Demoll, E. *Biochemistry* **1995**, *34*, 4617.
(164) Meyer, O.; Jacobitz, S.; Kruger, B. *FEMS Microbiol. Rev.* **1986**, *39*, 161.
(165) Gnida, M.; Ferner, R.; Gremer, L.; Meyer, O.; Meyer-Klaucke, W. *Biochemistry* **2003**, *42*, 222.
(166) Dobbek, H.; Gremer, L.; Kiefersauer, R.; Huber, R.; Meyer, O. *Proc. Natl. Acad. Sci. U.S.A.* **2002**, *99*, 15971.
(167) Bray, R. C.; George, G. N.; Lange, R.; Meyer, O. *Biochem. J.* **1983**, *211*, 687.
(168) Meyer, O.; Frunzke, K.; Mörsdorf, G. In *Microbial Growth on C_1 Compounds*; Murrell, J. C., Kelly, D. P., Eds.; Intercept, Ltd.: Andover, MA, 1993.
(169) Drennan, C. L.; Heo, J.; Sintchak, M. D.; Schreiter, E.; Ludden, P. W. *Proc. Natl. Acad. Sci. U.S.A.* **2001**, *98*, 11973.
(170) Doukov, T. I.; Iverson, T.; Seravalli, J.; Ragsdale, S. W.; Drennan, C. L. *Science* **2002**, *298*, 567.
(171) Dobbek, H.; Svetlitchnyi, V.; Gremer, L.; Huber, R.; Meyer, O. *Science* **2001**, *293*, 1281.
(172) Darnault, C.; Volbeda, A.; Kim, E. J.; Legrand, P.; Vernede, X.; Lindahl, P. A.; Fontecilla-Camps, J. C. *Nat. Struct. Biol.* **2003**, *10*, 271.
(173) Chen, J.; Huang, S.; Seravalli, J.; Gutzman, H., Jr.; Swartz, D. J.; Ragsdale, S. W.; Bagley, K. A. *Biochemistry* **2003**, *42*, 14822.
(174) DeRose, V. J.; Telser, J.; Anderson, M. E.; Lindahl, P. A.; Hoffman, B. M. *J. Am. Chem. Soc.* **1998**, *120*, 8767.
(175) Bertini, I.; Luchinat, C. In *Bioinorganic Chemistry*; Bertini, I., Gray, H. B., Lippard, S. J., Valentine, J. S., Eds.; University Science Books: Mill Valley, CA, 1994.
(176) Kim, E. J.; Feng, J.; Bramlett, M. R.; Lindahl, P. A. *Biochemistry* **2004**, *43*, 5728.
(177) Lindahl, P. A. *Biochemistry* **2002**, *41*, 2097.
(178) Kumar, M.; Lu, W.-P.; Liu, L.; Ragsdale, S. W. *J. Am. Chem. Soc.* **1993**, *115*, 11646.
(179) Seravalli, J.; Kumar, M.; Lu, W.-P.; Ragsdale, S. W. *Biochemistry* **1997**, *36*, 11241.
(180) Page, C. C.; Moser, C. C.; Chen, X. X.; Dutton, P. L. *Nature* **1999**, *402*, 47.
(181) Menon, S.; Ragsdale, S. W. *Biochemistry* **1996**, *35*, 15814.
(182) Bhatnagar, L.; Krzycki, J. A.; Zeikus, J. G. *FEMS Microbiol. Lett.* **1987**, *41*, 337.
(183) Santiago, B.; Meyer, O. *FEMS Microbiol. Lett.* **1996**, *136*, 157.
(184) Tan, X.; Loke, H. K.; Fitch, S.; Lindahl, P. A. *J. Am. Chem. Soc.* **2005**, *127*, 5833.
(185) Maynard, E. L.; Lindahl, P. A. *J. Am. Chem. Soc.* **1999**, *121*, 9221.
(186) Seravalli, J.; Ragsdale, S. W. *Biochemistry* **2000**, *39*, 1274.
(187) Ragsdale, S. W.; Wood, H. G.; Antholine, W. E. *Proc. Natl. Acad. Sci. U.S.A.* **1985**, *82*, 6811.
(188) Svetlitchnyi, V.; Dobbek, H.; Meyer-Klaucke, W.; Meins, T.; Thiele, B.; Romer, P.; Huber, R.; Meyer, O. *Proc. Natl. Acad. Sci. U.S.A.* **2004**, *101*, 446.
(189) Peters, J. W.; Lanzilotta, W. N.; Lemon, B. J.; Seefeldt, L. C. *Science* **1998**, *282*, 1853.
(190) Nicolet, Y.; Lemon, B. J.; Fontecilla-Camps, J. C.; Peters, J. W. *Trends Biochem. Sci.* **2000**, *25*, 138.
(191) Lindahl, P. A. *J. Biol. Inorg. Chem.* **2004**, *9*, 516.
(192) Brunold, T. C. *J. Biol. Inorg. Chem.* **2004**, *9*, 533.
(193) Riordan, C. *J. Biol. Inorg. Chem.* **2004**, *9*, 542.
(194) Drennan, C. L.; Doukov, T. I.; Ragsdale, S. W. *J. Biol. Inorg. Chem.* **2004**, *9*, 511.
(195) Seravalli, J.; Kumar, M.; Ragsdale, S. W. *Biochemistry* **2002**, *41*, 1807.
(196) George, S. J.; Seravalli, J.; Ragsdale, S. W. *J. Am. Chem. Soc.* **2005**, *127*, 13500.
(197) Schenker, R. P.; Brunold, T. C. *J. Am. Chem. Soc.* **2003**, *125*, 13962.
(198) Ragsdale, S. W.; Ljungdahl, L. G.; DerVartanian, D. V. *Biochem. Biophys. Res. Commun.* **1983**, *115*, 658.
(199) Shin, W.; Anderson, M. E.; Lindahl, P. A. *J. Am. Chem. Soc.* **1993**, *115*, 5522.
(200) Barondeau, D. P.; Lindahl, P. A. *J. Am. Chem. Soc.* **1997**, *119*, 3959.
(201) Seravalli, J.; Xiao, Y.; Gu, W.; Cramer, S. P.; Antholine, W. E.; Krymov, V.; Gerfen, G. J.; Ragsdale, S. W. *Biochemistry* **2004**, *43*, 3944.
(202) Ram, M. S.; Riordan, C. G. *J. Am. Chem. Soc.* **1995**, *117*, 2365.
(203) Ram, M. S.; Riordan, C. G.; Yap, G. P. A.; Liable-Sands, L.; Rheingold, A. L.; Marchaj, A.; Norton, J. R. *J. Am. Chem. Soc.* **1997**, *119*, 1648.
(204) Martin, B. D.; Finke, R. G. *J. Am. Chem. Soc.* **1990**, *112*, 2419.
(205) Menon, S.; Ragsdale, S. W. *Biochemistry* **1998**, *37*, 5689.
(206) Menon, S.; Ragsdale, S. W. *J. Biol. Chem.* **1999**, *274*, 11513.
(207) Lebertz, H.; Simon, H.; Courtney, L. F.; Benkovic, S. J.; Zydowsky, L. D.; Lee, K.; Floss, H. G. *J. Am. Chem. Soc.* **1987**, *109*, 3173.
(208) Ragsdale, S. W.; Wood, H. G. *J. Biol. Chem.* **1985**, *260*, 3970.
(209) Seravalli, J.; Gu, W.; Tam, A.; Strauss, E.; Begley, T. P.; Cramer, S. P.; Ragsdale, S. W. *Proc. Natl. Acad. Sci. U.S.A.* **2003**, *100*, 3689.
(210) Matthews, R. G. *Acc. Chem. Res.* **2001**, *34*, 681.
(211) Tan, X.; Sewell, C.; Yang, Q.; Lindahl, P. A. *J. Am. Chem. Soc.* **2003**, *125*, 318.
(212) Matthews, R. G. In *Vitamin B_{12}*; Banerjee, R., Ed.; John Wiley and Sons: New York, 1999; Vol. 1.
(213) Goulding, C. W.; Postigo, D.; Matthews, R. G. *Biochemistry* **1997**, *36*, 8082.
(214) Drennan, C. L.; Huang, S.; Drummond, J. T.; Matthews, R. G.; Ludwig, M. L. *Science* **1994**, *266*, 1669.
(215) Evans, J. C.; Huddler, D. P.; Hilgers, M. T.; Romanchuk, G.; Matthews, R. G.; Ludwig, M. L. *Proc. Natl. Acad. Sci. U.S.A.* **2004**, *101*, 3729.
(216) Dixon, M. M.; Huang, S.; Matthews, R. G.; Ludwig, M. *Structure* **1996**, *4*, 1263.
(217) Doukov, T.; Seravalli, J.; Stezowski, J.; Ragsdale, S. W. *Structure* **2000**, *8*, 817.
(218) Seravalli, J.; Shoemaker, R. K.; Sudbeck, M. J.; Ragsdale, S. W. *Biochemistry* **1999**, *38*, 5736.
(219) Seravalli, J.; Zhao, S.; Ragsdale, S. W. *Biochemistry* **1999**, *38*, 5728.
(220) Smith, A. E.; Matthews, R. G. *Biochemistry* **2000**, *39*, 13880.
(221) Peariso, K.; Goulding, C. W.; Huang, S.; Matthews, R. G.; Penner-Hahn, J. E. *J. Am. Chem. Soc.* **1998**, *120*, 8410.
(222) Myers, L. C.; Terranova, M. P.; Ferentz, A. E.; Wagner, G.; Verdine, G. L. *Science* **1993**, *261*, 1164.
(223) Huang, C. C.; Casey, P. J.; Fierke, C. A. *J. Biol. Chem.* **1997**, *272*, 20.
(224) Gray, H. B.; Winkler, J. R. *Proc. Natl. Acad. Sci. U.S.A.* **2005**, *102*, 3534.
(225) Liu, K. E.; Wang, D.; Huynh, B. H.; Edmondson, D. E.; Salifoglou, A.; Lippard, S. J. *J. Am. Chem. Soc.* **1994**, *116*, 7465.
(226) Valentine, A. M.; Wilkinson, B.; Liu, K. E.; Komar-Panicucci, S.; Priestley, N. D.; Williams, P. G.; Morimoto, H.; Floss, H. G.; Lippard, S. J. *J. Am. Chem. Soc.* **1997**, *119*, 1818.

CR0503153